Vibration Reduction of Marine Cable Systems Using Dynamic Absorbers

by

James E Tatera

B.S. Systems Engineering
United States Naval Academy, 1986

Submitted to the Department of Ocean Engineering in Partial Fulfillment of the
Requirements for the Degrees of

Naval Engineer

and

Masters of Engineering: Program in Marine Environmental Systems

at the
Massachusetts Institute of Technology
June 1996

© 1996 James E Tatera

The author hereby grants to MIT permission to reproduce and to distribute publicly paper
and electronic copies of this thesis in whole or in part.

Signature of Author:_____
Department of Ocean Engineering
May 10, 1996

Certified by:_____
J. Kim Vandiver
Professor of Ocean Engineering
Thesis Supervisor

Accepted by:_____
Prof. A. Douglas Carmichael
Chairman, Department Graduate Committee

19960919 027

Vibration Reduction of Marine Cable Systems Using Dynamic Absorbers

by

James E Tatera

Abstract

An engineering approach to the design of an in-line dynamic absorber is presented using transfer matrix techniques for an infinitely long cable system. The natural frequencies of the system are determined and the properties of the installed damper are optimized to maximize the amount of energy absorbed. Numerical simulations show that the optimally tuned and damped in-line dynamic absorber will dissipate 50% of incident transverse vibration energy. A design methodology for a nominal marine monitoring program is presented and specific engineering constraints provided to ensure that the modeled system meets design specifications

DEPARTMENT OF THE NAVY

NAVAL RESERVE OFFICERS TRAINING CORPS CONSORTIUM
BOSTON UNIVERSITY-M.I.T.

Massachusetts Institute of Technology
77 Massachusetts Ave Room 20E-125
Cambridge MA 02139-4307

Boston University
116 Bay State Road
Boston MA 02215-1796

IN REPLY REFER TO

1500
61:rjg
Ser 1079
29 Jul 1996

From: Comanding Officer, Boston University-MIT NROTC Consortium, Cambridge, MA
To: Director of Civilian Institutions Programs, Code 031, Naval Postgraduate School, 589 Dyer Road, Room 228, Root Hall, Monterey, CA 93943-5143
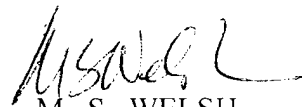
Ref: (a) NAVPGSCOLINST 1520.1D

Subj: END OF TOUR REPORTS

Encl: (1) End of Tour Reports
(2) Two Copies of Transcripts
(3) Two Copies of Thesis

1. The following students have graduated and completed the Educational Skill Requirements (ESR) necessary for award of a subspeciality code. Enclosures (1) - (3) are forwarded in accordance with reference (a).

Name	Curriculum	Subspeciality Code
LT Michael Amrozowicz	510	51N
LCDR John M. Barentine	510	51N
LCDR David R. Beckett	510	51N
LT Jess E. Riggle	510	51N
LT James E. Tatera	510	51N
LCDR Mark W. Thomas	510	51N
LCDR Bruce W. Brisson	520	52N
LCDR Thomas J. Moore	520	52N

M. S. WELSH
LCDR USN
By direction

Copy to:
Capt R. Tuddenham (SEA03R) w/ Encl (1) ,(Brisson, Moore)
PERS 445 w/o Encl
file

Acknowledgments

I would like to thank Professor J. Kim Vandiver, my thesis supervisor, for the guidance and support he has provided me throughout the year. Without his patient understanding, I would not be walking down Killian Court on June 7th, 1996.

I also would like to express my deepest thanks to my best friend and biggest supporter--my wife, Becky Tatera. With 5 years down and a lifetime to go, I wonder every day how I can be so lucky. From the hectic summer days in 1993 to these final crazy days in 1996, you have made this experience special. Thank you for being there for me.

Contents

Chapter 1

Introduction

Investigation of the marine environment is a growing industry. In order to economically obtain enough information, increased usage of remote sensing technologies will be required. The use of these technologies will require that such information collection systems be robust enough to survive in the harsh environment for prolonged periods of time without human intervention. In most cases, the areas of concern for the scientist can be defined by a geographical boundary, and an ocean mooring can be used to locate the measuring devices. The motions of the moored body can damage the equipment or produce erroneous readings. Thus, the robust requirement of the measurement system will lead to either a hardening of the sensitive electronics of the system or other some other sort of isolation method that will decrease the cyclic loading that will be seen by the system.

The problem of the motion of a moored buoy with sensitive electronic instruments located along the length of the cable can be modeled as a string with a rigid lumps. A previous analytical approach of the problem was performed by Li [1]. In his analysis, Li was able to provide a analytical description of how to model a string/rigid lump system by the geometric and material properties of the components and the cable and consider the system more than just a lumped mass at a particular point along the cable. The energy of the wave traveling along the cable might be transmitted through the component or reflected back, depending upon the specifics of the problem.

If the physical connection of the equipment along the length of the cable were to include a spring and a damper, the model becomes more complex. The energy of the wave traveling along the cable might then be absorbed, transmitted or reflected at the interface, dependent upon the nature of the system and the frequency of the incoming wave. Li was able to investigate the modeling of a mass/string/damper system that would

be installed along the line, as well as endpoint terminations of the cable—either connected to a moving or a fixed frame of reference. The in-line system has more of a practical application as it can become a part of the device itself, as components may be changed along the length of a moored cable in order to alter the measurement systems available to the scientist in the field.

The idea that the in-line component could be isolated via an appropriately engineered system has significant applications. The component then could be designed more towards the gathering of information, not just being able to withstand the normal marine forces. Using the ideas established by Li, this thesis will investigate the characteristics of such a moored body system and develop an engineering approach to determining the optimum value of the constituent parts of the measurement devices such that the operation of the in-line components is not impaired.

This thesis will investigate the design of an in-line dynamic absorber tuned to the frequency where the maximum amount of energy traveling along the ocean mooring system can be absorbed. Chapter 2 outlines the rationale that drives the need for this analysis. Additionally, an application that presents a process for the design of a marine monitoring program and establishes technical requirements is introduced.

Chapter 3 is the introduction to the use of transfer matrix notation and the benefits that result in the use of this system. Chapter 4 is the analysis section of this thesis. The search for an analytical approach to determining the optimum amount of energy that can be absorbed in the mooring system is provided. A numerical result is obtained and the optimum value for the absorber for a given system is provided. Chapter 5 is a discussion of the major findings and potential areas for further research.

Chapter 2

Oceanographic Monitoring System

2.1 Introduction

The design process to implement an oceanographic monitoring system discussed in chapters 1 must minimize the effects of marine induced forces on an infinitely long cable system with installed monitoring equipment. One practical application of the design process will involve the use of a monitoring system that is located in a marine environment of interest. This chapter will describe how such a monitoring plan is designed and implemented.

The first step in the development of a monitoring plan requires an executive level design methodology. Using the concepts from a report by the National Research Council [2], the following steps are used:

1. Define Expectations and Goals
2. Define Study Strategy
3. Conduct Exploratory Studies if Needed
4. Develop Sampling Design
5. Implement Study

The expectations and goals of the particular monitoring plan would be based upon the marine site chosen. The ultimate goal is to have a monitoring system that produces useful information that can used to make a reasoned decision. Thus, the effects that are seen in the monitoring results must reflect information about the situation that exists in the marine environment. The legal framework that guides the administration of human actions in the marine environment also molds the expectations and goals of the monitoring plan.

Defining the study strategy of the monitoring plan requires the implementation of a strategy that begins with the identification of resources in the marine environment that are at risk. From that identification, a conceptual model is developed that establishes links that exist in the marine ecosystem components. These links involve spatial, temporal, biological and chemical variables that become the basis of the study strategy. Feedback

among the monitored variables in the plan might dictate that some be changed to better reflect the marine environment. The inherent uncertainties of a conceptual model must also be considered in the definition of the study strategy. The final result is a set of questions concerning the marine environment that can be tested to describe the state of the marine environment.

Exploratory studies that have been performed on similar marine ecosystems can be used as a basis for the monitoring plan. If the need exists to validate certain technical issues such as the measurement of parameters under various hydrodynamic conditions (for a coastal system, high river flow from spring melt of snow or low river flow from a period of no precipitation), preliminary studies should be performed. The primary research performed for this validation becomes an interdependent part of the monitoring plan, altered as the need arises to obtain specific information.

The development of a sampling plan uses the testable questions described previously in the study plan and identifies meaningful levels of changes that can be measured. In the establishment of these meaningful levels of change, the natural variability of the marine environment in question needs to be considered. A meaningful level of change must also be established that will be observable in a time frame that allows a reasoned decision to be made that will have an impact on the system being measured. This definition of meaningful change will also be as fluid as the improvement of prediction models and the analysis of data will allow. The selection of the variables to measure in the monitoring plan is limited by the resources available, and they must be chosen to provide the most useful information about the status of the system. Thus, variables may be measured that will provide a realistic view of the system, although they may not be part of the predictive model. These substitute variables may contain early warning signs of system degradation or information concerning specific items of interest to the users of the sampling plan. In either case, the substitute variables will provide information that can be applied to the predictive model via knowledge of the interactions between the substitute variables and the model variables. The use of specific oceanographic measurement equipment is then chosen to reflect the variables measured.

8

Two concerns that must be addressed in the design of the sampling plan are the level of confidence in the knowledge of the interactions among the elements of the system and the statistical characteristics of the sampling of the designated variables. If the interactions among the biological elements is purely theory, then the uncertainty must be addressed in the analysis. If the sampling process requires a significant number of samples in order to verify the validity of the measurement, then the monitoring plan is not efficient in obtaining the maximum amount of information for the effort.

Using the concepts described in the preceding paragraphs, the monitoring plan will be implemented, with constant feedback to ensure that the model, the sampling plan and the uncertainty of the monitoring plan are all considered when updating the process.

2.2 Tiered System Structure

Using the guidelines for establishing a monitoring plan described above leads to a variety of monitoring plans based upon conditional aspects of the system being studied. An approach used by a team of graduate students at MIT [9]. provided a tiered system approach to a monitoring plan that allows a manager to best allocate the available resources when developing the monitoring plan.
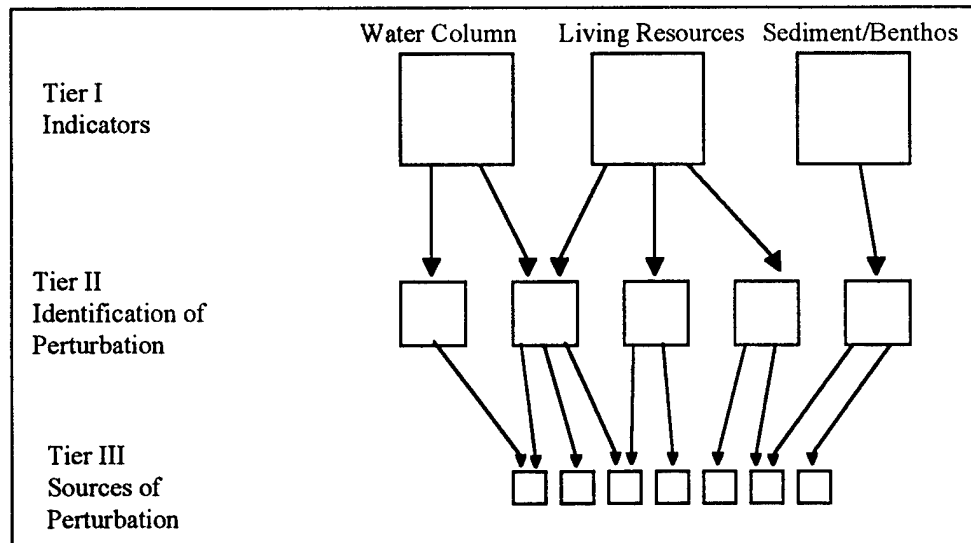
Figure 2- 1: Three Tiered Strategy

9

The tiered structure is classified to characterize three potential areas of impact within a monitoring plan area. Those areas are: 1) Water Column Region, 2) Living Resources , and 3) Sediment/Benthos. The monitoring plan addresses these three areas in three tiered levels of measurement. The three tiered strategy is graphically represented in figure 4-1. Each box represents a variable that is part of the generic design study. The number of the boxes would change based upon the specific application The arrows represent that the tiers are logically linked to each other. Note that the logical links from one tier to the next may indicate more than one cause and effect relationship for a particular variable.

The first tier in the monitoring structure is comprised of variables that react quickly to the changes in the marine system, and provide advanced warning of potential events. Tier I items include the measurement of water quality variables, such as temperature, salinity and dissolved oxygen in the water column. The living resources classification is measured in fish population studies for tier I. The benthos region tier I measurements include bottom observations that may be made with remote sensing equipment.

If the variables measured in the first tier exceed a threshold value, then more extensive analysis must be performed. This triggers the investigation of the tier II variables via a logical link to the most probable source of the perturbation. The tier II variables require a more complex analysis that is generally more expensive and not be performed *in situ*. An example of a tier II variable is the chemical analysis of the water column that requires a grab sample be obtained and transported to a laboratory. The living resources tier II variable would be the analysis of animal or plant material to determine its make-up and compare it to standard information. A tier II benthos region variable would again be a chemical analysis of the material of the sediment.

The final portion of the tiered system is the logical link from the identification of the perturbation to the most probable source of the change. This involves the tracing of the cause of the perturbation to its source. The basis for this would be set up in the design study, when potential sources of perturbation to the marine system would be identified as

10

any facility that could potentially add material and or heat to the region around the boundary of the marine system being monitored (power plants, industrial plants, chemical plants). This detective effort is the final result of the monitoring plan because it is the information that managers need to form their reasoned opinions concerning liability and potential litigation.

The most significant advantage of the three tiered system is its modularity. The system can promptly be updated to reflect the information obtained when the monitoring system goes into effect. Additionally, the three classifications of water column, living resources and benthos/sediment characterize the essential aspects of the marine environment. Each tier can be expanded horizontally as information is obtained and more classifications can be added if required. If additional links are provided with the improvement in knowledge, the links can also be updated.

The modularity of the system allows the resource manager to best use the assets that are available if the entire plan can not be fully implemented. The logical links that connect the tiers describe flow paths that can be chosen in either a bottom up or top down approach to investigate the potential cause and effect relationships.

2.3 Implementation

The use of moored oceanographic systems to measure components that are part of the monitoring plan will likely be used because of the cost effectiveness of remote sensing and the possibility of real time data management from a shore based office. In order to technically achieve the use of moored oceanographic systems, it is imperative that external forcing functions that move the system be controlled to allow sensitive equipment to operate without damage.

The use of the design process to design a dynamic absorber can be used most effectively in the tier I analysis of the monitoring plan. The vision is that the particular measurement desired to be measured in the water column *in situ* can be designed to operate installed on a moored buoy system. The power source for the system can be designed to last for a designated period of time that the user would correspond to a

11

maintenance schedule for the equipment. Current renewable energy systems rely on solar energy or other means that would be installed in the moored system near the free surface that would suffer if excess drag or vibrations caused the buoyant portion of the moored system to go underwater. Communications with the land based researchers would also be connected to the installed devices via the mooring cable. This communication suite would most likely be installed in a buoyant body near the free surface in a vulnerable position.

A specific example of a typical oceanographic system would include acoustic transducers to monitor various components of the marine environment. These transducers are very sensitive to excessive vibrations, and the design process to remove as much vibration energy from the system as possible would help to ensure that the installed equipment could operate properly.

With the implementation of Autonomous Underwater Vehicles (AUVs) in the marine environment, certain tier II variables can also be measured. Ongoing work within the Ocean Engineering Department at MIT is investigating the implementation of new technology that will greatly reduce the amount of power required to operate the propulsion systems of AUVs. The computer program required in order to operate an AUV in the underwater marine environment has also been the subject of recent studies at MIT. The power and communication source for the AUV would be connected to another moored cable system that would have an underwater docking port. This docking port would provide the communications link with the land based researchers and replenish the power used in the tier II investigations.

Of particular concern to each of the applications described above is the principal of flow induced vibrations. Even with a steady current moving past a cable system or a cable system being towed by a vessel at a constant speed, oscillatory motions are induced when vortex shedding occurs on the cable. The motions of the cable are dominated by motions that are transverse to the direction of the flow and occur at a frequency equal to the vortex shedding frequency. In-line motions occur at twice the vortex shedding frequency, and are not considered in this analysis because of their small contribution to the cable motion.

The vortex shedding excitation frequency often coincides with a resonant frequency of the cable and results in substantial response.

The non-dimensional parameter that characterizes the frequency of vortex shedding is the Strouhal number, and the typical value associated with it is .21 and it is constant over a wide range of Reynolds number. [4]. The expression relating the Strouhal number and the vortex shedding frequency is:

$$\omega = \frac{St \cdot V}{d} \cdot 2 \cdot \pi$$

EQN 2- 1

Where ω is the angular frequency, V is the velocity of the cable being towed or the current flowing past the cable, and d is the diameter of the cable. In the design process, a limit needs to be established for reasonable expectations of vortex shedding frequencies that the moored system may face. Assuming a limit of a 5 knot current (2.54 m/sec) and a range of cable diameters from 1/4 inch to 1 inch, Figure 2-2 represents the expected vortex shedding frequencies.
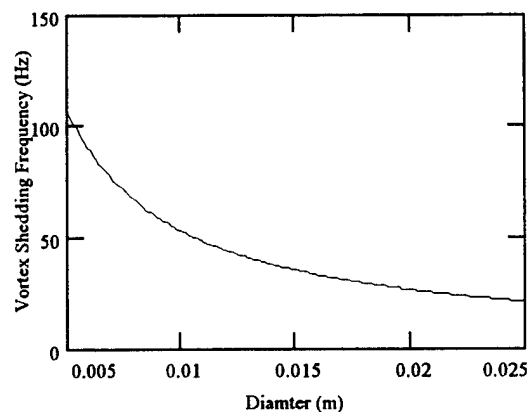
Figure 2- 2: Vortex Shedding Excitation Frequencies in a 2.5 m/sec Current

In addition to this vibrational lock in of the cable, an additional concern for flow induced vibration is the increase in the nondimensional drag coefficient, CD. This increase in drag has major implication to mooring design.

13

Understanding the need for the oceanographic monitoring and the environment in which the components will be operated leads directly to an investigation to reduce the amount of energy that the installed components will see. This investigation to limit the effect of the ocean loading, in particular the vortex-induced vibrations, is pursued using an in-line dynamic absorber.

Chapter 3

Transfer Matrix Evaluation

3.1 Background

The transfer matrix method is a technique to evaluate a complicated system through the use of discrete transformations from one location to another. For a sequential system of cable, rigid bodies, springs and dampers, the final system transfer matrix is the product of each transfer matrix from one location to the other. The benefit of this system is the ability to evaluate the response of a complicated system through sequential multiplication of finite transfer matrices from point to point. The analysis of this thesis will evaluate the transfer matrix for an oceanographic moored system with a damping connector installed in-line, shown in Figure 4-1.

Using the transfer matrix method requires that a state vector be defined. The state vector is comprised of Fourier transforms of displacements and the corresponding internal forces [5]. In the case of a cable system with installed masses, springs and dampers, the state vector is described by:

$$z_i = \begin{bmatrix} \overline{y} \\ \overline{Ty'} \end{bmatrix}_i \qquad \text{EQN 3-1}$$

where $\overline{y}$ is the Fourier transform of the displacement of the system, $\overline{y'}$ is the Fourier transform of the rotation of the system, and T is the tension of the system. All three items are evaluated at the particular point (annotated by the subscript i), and the transformation from one location to the next is defined by:

$$z_i = A_i z_{i-1} \qquad \text{EQN 3-2}$$

where the transfer matrix A_i links the two state vectors.

15

3.2 Derivation of a Transfer Matrix

The determination of the transfer matrix is based upon an analytical description of the cable system. This thesis uses the transfer matrix library determined by Li.[1]. In order to describe how the transfer matrices are established, an alternate description of an equivalent system is provided. Knowing the geometric relationships and determining the equations of motion are the keys to deriving the transfer matrix for a system.
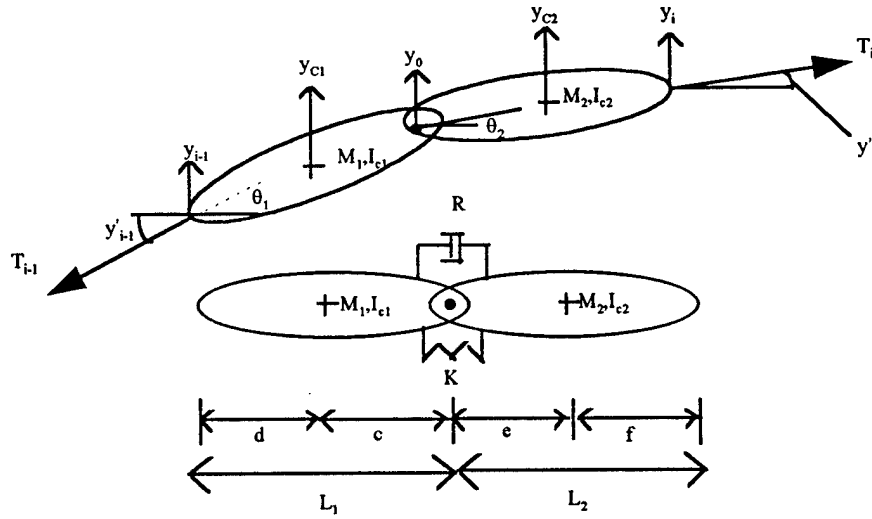
Figure 3-1: Schematic of System

Using figure 3-1 and setting $M_1 = M_2 = M$, the following equations of motion can be described in the y direction:

$$M\ddot{y}_{c2} = T_i y_i' - T_{oy}$$
$$\underline{+M\ddot{y}_{c1} = T_{oy} - T_{i-1}y_{i-1}'}$$
$$M(\ddot{y}_{c2} + \ddot{y}_{c1}) = T_i y' - T_{i-1}y_{i-1}'$$

EQN 3- 3

Where T_{oy} is the internal force at the joint located at y_0 acting in the y_0 direction

The equations for summation of moments about the center of gravity of the two links are described by the following:

16

$$I_{c2}\ddot{\theta}_2 = K_\theta(\theta_1 - \theta_2) + R_\theta(\dot{\theta}_1 - \dot{\theta}_2) + T_i(y_i' -_i \theta_2)f \qquad \text{EQN 3- 4}$$

$$I_{c1}\ddot{\theta}_1 = K_\theta(\theta_2 - \theta_1) + R_\theta(\dot{\theta}_2 - \dot{\theta}_1) + T_{i-1}(y_{i-1}' - \theta_1)d \qquad \text{EQN 3- 5}$$

Where K_θ is the value of the torsional spring constant (Nm/rad) and R_θ is the value of the torsional damping constant (Nm/(rad/sec)).

If the following geometric relations:

$$y_{c1} = \frac{c}{L_1}y_{i-1} + \frac{d}{L_1}y_o \qquad \text{EQN 3- 6}$$

$$y_{c2} = \frac{f}{L_2}y_0 + \frac{e}{L_2}y_i \qquad \text{EQN 3- 7}$$

are inserted in Equation 3-3, we obtain:

$$\ddot{y}_0 = \frac{L_1}{(d+f)M}(T_i y_i' - T_{i-1}y_{i-1}') - \frac{L_1}{(d+f)}(\frac{c}{L_1}\ddot{y}_{i-1} + \frac{e}{L_2}\ddot{y}_i) \qquad \text{EQN 3- 8}$$

And if we substitute the following angular relationships:

$$\theta_1 = \frac{y_0 - y_{i-1}}{L_1} \quad \text{and} \quad \theta_2 = \frac{y_i - y_0}{L_2} \qquad \text{EQN 3- 9}$$

into equations 3-4 and 3-5, we obtain:

$$I_{c2}\frac{(\ddot{y}_i - \ddot{y}_0)}{L_2} = K_\theta(\frac{y_0 - y_{i-1}}{L_1} - \frac{y_i - y_0}{L_2}) + R_\theta(\frac{\dot{y}_0 - \dot{y}_{i-1}}{L_1} - \frac{\dot{y}_i - \dot{y}_0}{L_2}) + T_i(y_i' - \frac{y_i - y_0}{L_2})f$$

$$\text{EQN 3- 10}$$

and

$$I_{c1}\frac{\ddot{y}_0 - \ddot{y}_{i-1}}{L_1} = K_\theta(\frac{y_i - y_0}{L_2} - \frac{y_0 - y_{i-1}}{L_1}) + R_\theta(\frac{\dot{y}_i - \dot{y}_0}{L_2} - \frac{\dot{y}_0 - \dot{y}_{i-1}}{L_1}) + T_{i-1}(y_{i-1}' - \frac{\dot{y}_0 - \dot{y}_{i-1}}{L_1})d$$

$$\text{EQN 3- 11}$$

17

Performing the Fourier transform of Equation 3-8 and setting $T_i = T_{i-1} = T$, $d = f = l_2$, $c = e = l_1$, and $L_1 = L_2 = L$, we obtain:

$$\overline{y}_0 = -\frac{1}{\omega^2}\frac{TL}{2l_2}\left[\overline{y'}_i - \overline{y'}_{i-1}\right] - \frac{l_1}{2l_2}(\overline{y}_{i-1} + \overline{y}_i)$$ EQN 3-12

Where $\overline{y}_0$, $\overline{y}_{i-1}$, $\overline{y}_i$, $\overline{y'}_{i-1}$, and $\overline{y'}_i$ are the Fourier transforms of the displacements and the slopes at the particular locations.

Performing the Fourier transform of Equation 3-10 and $I_{c2} = M\kappa^2$ (κ is the radius of gyration), we obtain:

$$M\kappa^2(-\omega^2)\frac{1}{L}(\overline{y}_i - \overline{y}_0) = K_\theta \frac{2\overline{y}_0 - (\overline{y}_{i-1} + \overline{y}_i)}{L} + \frac{R_\theta j\omega[2\overline{y}_0 - (\overline{y}_{i-1} + \overline{y}_i)]}{L} + T(\overline{y'}_i - \frac{\overline{y}_i - \overline{y}_0}{L})l_2$$ EQN 3-13

Performing the Fourier transform of Equation 3-11, and setting $I_{c1} = M\kappa^2$ (κ is the radius of gyration), we obtain:

$$M\kappa^2(-\omega^2)\frac{1}{L}(\overline{y}_0 - \overline{y}_{i-1}) = K_\theta \frac{\overline{y}_{i-1} + \overline{y}_i - 2\overline{y}_0}{L} + \frac{R_\theta j\omega(\overline{y}_{i-1} + \overline{y}_i - 2\overline{y}_0)}{L} + T(\overline{y'}_{i-1} - \frac{\overline{y}_0 - \overline{y}_{i-1}}{L})l_2$$ EQN 3-14

If we substitute Equation 3-12 into Equation 3-13 and rewrite, we obtain:

$$A_1\overline{y}_i + B_1\overline{y'}_i = C_1\overline{y}_{i-1} + D_1\overline{y}_{i-1}$$ EQN 3-15

Where:

$$A_1 = \frac{-M\kappa^2\omega^2}{L}(1 + \frac{l_1}{2l_2}) + \frac{K_\theta}{L} + \frac{l_1 K_\theta}{Ll_2} + \frac{j\omega R_\theta}{L} + \frac{l_1 R_\theta j\omega}{Ll_2} + \frac{l_2 T}{L} + \frac{l_1 T}{2L}$$

$$B_1 = \frac{-M\kappa^2 T}{2l_2} + \frac{TK_\theta}{l_2\omega^2} - \frac{R_\theta T}{j\omega l_2} - Tl_2 + \frac{T^2}{2\omega^2}$$

$$C_1 = \frac{M\kappa^2\omega^2}{2Ll_2}l_1 - \frac{K_\theta}{L} - \frac{l_1 K_\theta}{Ll_2} - \frac{j\omega R_\theta}{L} - \frac{l_1 R_\theta j\omega}{Ll_2}$$

18

$$D_1 = \frac{M\kappa^2 T}{2l_2} - \frac{TK_\theta}{l_2\omega^2} - \frac{R_\theta T}{j\omega l_2} - \frac{Tl_1}{2L} + \frac{T^2}{2\omega^2}$$

And combining Equations 3-13 and 3-14 and rewriting to obtain:

$$A_2 \overline{y}_i + B_2 \overline{y}_i = C_2 \overline{y}_{i-1} + D_2 \overline{y}_{i-1}$$ EQN 3- 16

Where

$$A_2 = \frac{-M\kappa^2\omega^2}{L} + \frac{Tl_2}{L} \quad \text{and} \quad B_2 = -Tl_2 \quad \text{and} \quad C_2 = \frac{-M\kappa^2\omega^2}{L} - \frac{Tl_2}{L} \quad \text{and} \quad D_2 = Tl_2$$

The final equations for the transfer function can be formed using the following relationship:

$$\begin{bmatrix} \overline{y}_i \\ \overline{Ty'}_i \end{bmatrix} = \begin{bmatrix} t_{11} & t_{12} \\ t_{21} & t_{22} \end{bmatrix} \begin{bmatrix} \overline{y}_{i-1} \\ \overline{Ty'}_{i-1} \end{bmatrix}$$

Thus:

$$t_{11} = \frac{B_2 C_1 - B_1 C_2}{A_1 B_2 - A_2 B_1} \qquad\qquad t_{12} = \frac{1}{T}\frac{B_2 D_1 - B_1 D_2}{A_1 B_2 - A_2 B_1}$$

$$t_{21} = T\frac{A_1 C_2 - A_2 C_1}{A_1 B_2 - A_2 B_1} \qquad\qquad t_{22} = \frac{A_1 D_2 - A_2 D_1}{A_1 B_2 - A_2 B_1}$$ EQN 3- 17

Using the methods of transfer matrix operations allow an efficient calculation of important parameters such as the amount of energy that is reflected, absorbed or transmitted through a system. The analysis in the next chapter will provide that information and the techniques needed in order to reduce the amount of flow-induced vibrations that are seen in the system

19

Chapter 4

In-line Dynamic Absorber

4.1 System Description

Using the principles described in chapter 3, the transfer matrix formulation for a specific system can be described and studied. The system studied is a hinged connection of two rigid lump masses connected with a linear translational spring and damper connected in an infinitely long cable, shown in figure 4-1. The cable is aligned horizontally and the tensions are assumed to be constant along the cable.
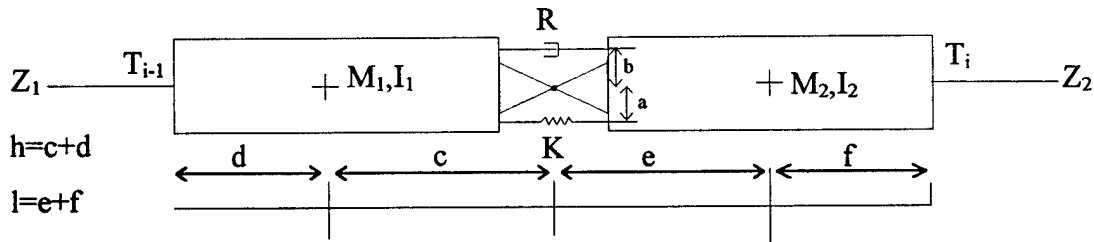
Figure 4- 1: Diagram of System

Where the relationship between the torsional components defined in chapter 3 and the linear translational components described here are given by the following:

$$K_\theta = Ka^2 \qquad \text{and} \qquad R_\theta = Rb^2 \qquad\qquad \text{EQN 4- 1}$$

An incident wave traveling along the cable can be described by:

$$A_i e^{-jkx} e^{j\omega t} \qquad\qquad \text{EQN 4- 2}$$

where A is the amplitude, k the wave number and ω the radial frequency of the wave. The subscript i corresponds to the incident wave.

When the incident wave encounters a discontinuity along the cable, the wave can be reflected or transmitted through the region. A comparison of the wave amplitudes provides the following:

$$T_c = \frac{A_t}{A_i} \quad \text{and} \quad R_c = \frac{A_r}{A_i} \qquad \qquad \text{EQN 4- 3}$$

where T_c is the transmission coefficient and R_c is the reflection coefficient.

Knowing the rate at which energy is carried by an incident wave along the cable is defined by

$$E = \frac{1}{2}\rho_c C \omega^2 A^2 \qquad \qquad \text{EQN 4- 4}$$

Where ρ_c is the linear density of the cable, C is the wave speed, ω is the frequency and A is the amplitude of the wave.

When the wave encounters the system shown in figure 4-1, the energy of the wave can be reflected, transmitted, or absorbed into the damper between the two masses. The energy of the waves that reflect back from the system can be determined as well as the energy of the waves that transmit through the system. The remaining energy, if any, represents the energy absorbed by the system, considering that energy must be conserved. The ratio of these energies are described by

$$\beta = \frac{E_r}{E_i} \quad \text{alternatively} \quad \beta = \left(\frac{A_r}{A_i}\right)^2 \qquad \qquad \text{EQN 4- 5}$$

and

$$\gamma = \frac{E_t}{E_i} \quad \text{alternatively} \quad \gamma = \frac{Z_2}{Z_1}\left(\frac{A_t}{A_i}\right)^2 \qquad \qquad \text{EQN 4- 6}$$

therefore

$$\alpha = \frac{E_a}{E_i} \quad \text{alternatively} \quad \alpha = 1 - \beta - \gamma \qquad \qquad \text{EQN 4- 7}$$

where the subscript i stands for incident, r stands for reflected, t stands for transmitted, and a stands for absorbed.

But the reflected and transmitted power ratios can also be described in terms of the reflection and transmission coefficients (equation 4-3).

21

$$\beta = |R_c|^2 \text{ and } \gamma = \frac{Z_2}{Z_1}|T_c|^2 \qquad \textbf{EQN 4- 8}$$

where α is still described as in equation 4-7 .

4.2 Resonance Frequencies

The first step of the analysis is to determine the frequency at which the system would have the maximum amount of energy absorption. This occurs at a frequency when the reflection coefficient is zero, thus all of the energy is either transmitted or absorbed. Using the elements of the transfer matrix, the expression for the reflection coefficient is provided by:

$$R_c(\omega) := \frac{-\left[\left(t_{21}(\omega)\right)+(\omega)^2 \cdot Z_1 \cdot Z_2 \cdot t_{12}(\omega)\right]+j \cdot \omega \cdot \left(Z_1 \cdot t_{22}(\omega)-Z_2 \cdot t_{11}(\omega)\right)}{t_{21}(\omega)-(\omega)^2 \cdot Z_1 \cdot Z_2 \cdot t_{12}(\omega)+j \cdot \omega \cdot \left(Z_1 \cdot t_{22}(\omega)+Z_2 \cdot t_{11}(\omega)\right)} \qquad \textbf{EQN 4- 9}$$

Where the elements of the square transfer matrix are $t_{ij}(\omega)$, for i and j equal to 1 to 2 and the impedance of the input and output cable are Z_1 and Z_2, respectively.

In addition to the reflection coefficient, the transmission coefficient can also be expressed in terms of the transfer matrix. The expression for the transmission coefficient is provided by:

$$T_c(\omega) := \frac{j \cdot 2 \cdot \omega \cdot Z_1}{t_{21}(\omega)-(\omega)^2 \cdot Z_1 \cdot Z_2 \cdot t_{12}(\omega)+j \cdot \omega \cdot \left(Z_1 \cdot t_{22}(\omega)+Z_2 \cdot t_{11}(\omega)\right)} \qquad \textbf{EQN 4- 10}$$

Reducing the expression for the reflection coefficient aids in the location its zeros:

$$Rc(\omega) = \frac{\left(-t_{21}(\omega)^2+\omega^4 \cdot Z_1^2 \cdot Z_2^2 \cdot t_{12}(\omega)^2+\omega^2 \cdot Z_1^2 \cdot t_{22}(\omega)^2-\omega^2 \cdot Z_2^2 \cdot t_{11}(\omega)^2+2i \cdot \omega \cdot Z_1 \cdot t_{22}(\omega) \cdot t_{21}(\omega)+2i \cdot \omega^3 \cdot Z_1 \cdot Z_2^2 \cdot t_{11}(\omega) \cdot t_{12}(\omega)\right)}{\left(t_{21}(\omega)^2-2 \cdot t_{21}(\omega) \cdot \omega^2 \cdot Z_1 \cdot Z_2 \cdot t_{12}(\omega)+\omega^4 \cdot Z_1^2 \cdot Z_2^2 \cdot t_{12}(\omega)^2+\omega^2 \cdot Z_1^2 \cdot t_{22}(\omega)^2+2 \cdot \omega^2 \cdot Z_1 \cdot t_{22}(\omega) \cdot Z_2 \cdot t_{11}(\omega)+\omega^2 \cdot Z_2^2 \cdot t_{11}(\omega)^2\right)}$$

$$\textbf{EQN 4- 11}$$

The numerator of this expression can be solved for values of ω such that it equals zero. These values of ω are the frequencies at which there is no reflection and the system has the potential for maximum energy absorption.

A second method of calculating the frequencies of the zeros of the reflection involves the use of the input impedance, defined by:

$$Z_m = \frac{force}{velocity} \quad \text{and} \quad Z_m(\omega) := \frac{t_{21}(\omega) + j \cdot \omega \cdot Z_2 \cdot t_{11}(\omega)}{-\omega^2 \cdot Z_2 \cdot t_{12}(\omega) + j \cdot \omega \cdot t_{22}(\omega)}$$

EQN 4- 12

By using the principal of impedance matching, the values of ω such that the imaginary part of this impedance is zero will provide the values of the frequencies where the potential for maximum energy absorption will occur. This leads to:

$$\text{Imaginary part of } \ Z_m(\omega) = \frac{-\omega^3 \cdot Z_2^2 \cdot t_{11}(\omega) \cdot t_{12}(\omega) - t_{21}(\omega) \cdot \omega \cdot t_{22}(\omega)}{\omega^4 \cdot Z_2^2 \cdot t_{12}(\omega)^2 + \omega^2 \cdot t_{22}(\omega)^2}$$

EQN 4- 13

The numerator of this expression can also be solved in order to find the values of ω such that the expression equals zero. These values are the resonance frequencies of the system.

**Table 4- 1: Input Values for the Determination of the Reflection Coefficient Zeros**

Characteristic	Value		Characteristic	Value
a	.0254 m		b	.0254 m
d	.1524 m		f	.1524 m
c	.1778 m		e	.1778 m
M_1	4.52 kg		M_2	4.52 kg
I_1	.035		I_2	.035 kgm^2
ρ_1	1.144 kg/m		ρ_2	1.144 kg/m
T_{i-1}	1000 newton		T_i	1000 newton
K	10 newton/m		R	0 newton/(m/sec)
H	1000 newton			

An analytic approach and a corresponding numerical solution to this problem is outlined in Appendix A. With the value of the damper set to zero, a numerical solution

can be obtained for both the zeros of the input impedance expression and the reflection coefficient expression. A numerical solution to this problem requires the input of characteristic values of the physical parameters of the system. In order to compare the simulation with a real world model of a cable system modeled by Vandiver [6], the values of the system shown in Figure 4-1 were set in accordance with Table 4-1.

The specific values shown in Table 4-1 represent a real world example of some oceanographic mooring components. Using these characteristic properties, a computer simulation of the system was conducted and the value of the frequencies of the zeros of the reflection coefficient were obtained using the secant method. The resulting values were $\Omega_1 = 42.6$ rad/sec and $\Omega_2 = 94.1$ rad/sec. Using the impedance method, the same values were obtained. The values of the reflection coefficient and the transmission coefficient are plotted in Figure 4-2.
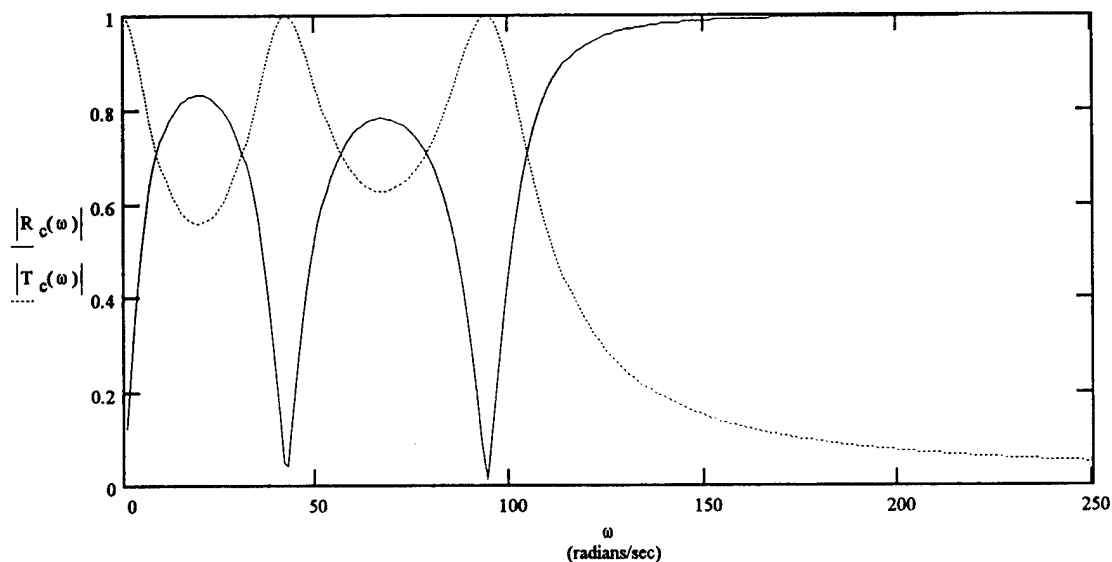
Figure 4- 2: Graph of Reflection and Transmission Coefficients Using Input Parameters from Table 4-1 (R=0)

For the curve shown in figure 4-2, the value of the damper was set at zero to observe the location of the minimum values of the reflection coefficient with no energy being absorbed in the system to aid in determining a starting value for the secant method

24

analysis. The location of these minimum values is not affected by a change in the damper value, R, although the values of the reflection and transmission coefficients are. This is shown in Figure 4-3, by increasing the damper to 500 N/(m/sec). The difference represents the amount of energy that is absorbed in the system.
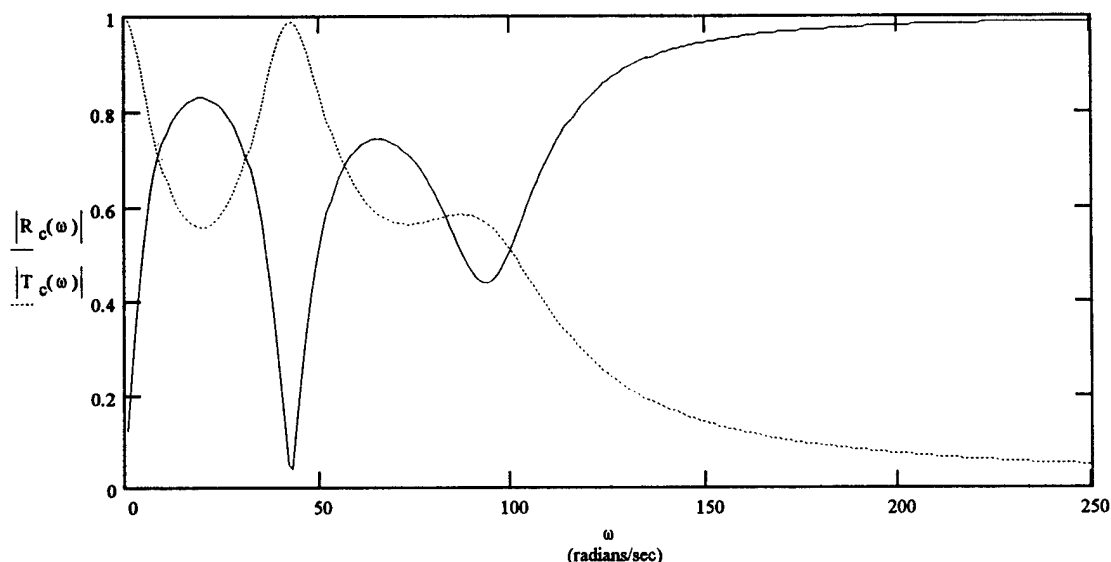
Figure 4- 3: Graph of Reflection and Transmission Coefficients Using Input Parameters from Table 4-1 (R=500 N/(m/sec))

4.3 Optimum Value for the Damper

The determination of the optimum value of a damper to absorb the maximum value of energy is frequency dependent. The maximum amount of energy will be absorbed at the resonance frequencies determined in the previous section. Using the two resonance frequencies as a basis, a search was conducted to determine this optimum damper value using the same expressions outlined in Appendix B. This time, however, all of the equations are dependent upon the value of a particular damper with the frequency held constant at either Ω_1 or Ω_2. This investigation emphasizes the higher resonance frequency because there is more relative motion between the two masses that leads to more energy absorption in the damper as seen in the modal sketch in Appendix A.

In order to determine the value of the damper that will lead to the maximum amount of energy absorbed for a particular frequency, the absorption power ratio must be analyzed. Using equation 4-6, the derivative of the absorption power coefficient with respect to R is described by:

$$\frac{\delta\alpha}{\delta R} = -\frac{\delta\beta}{\delta R} - \frac{\delta\gamma}{\delta R}$$

EQN 4- 14

Substituting equation 4-7 into equation 4-13, the following is obtained:

$$\frac{\delta\alpha}{\delta R} = \frac{-\delta\left(R_c \cdot \overline{R_c}\right)}{\delta R} - \frac{\delta\left(\dfrac{Z_2}{Z_1} \cdot T_c \cdot \overline{T_c}\right)}{\delta R}$$

EQN 4- 15

Which can be rewritten as:

$$\frac{\delta\alpha}{\delta R} = -\left(\frac{\delta R_c}{\delta R}\cdot \overline{R_c} + R_c \cdot \frac{\overline{\delta R_c}}{\delta R}\right) - \frac{Z_2}{Z_1}\cdot\left(\frac{\delta T_c}{\delta R}\cdot \overline{T_c} + T_c \cdot \frac{\overline{\delta T_c}}{\delta R}\right)$$

EQN 4- 16

Because the order of the partial derivative operation and the complex conjugate calculation are interchangeable, the final expression can be rewritten as:

$$\frac{\delta\alpha}{\delta R} = -\left(\frac{\delta R_c}{\delta R}\cdot \overline{R_c} + R_c \cdot \overline{\left(\frac{\delta R_c}{\delta R}\right)}\right) - \frac{Z_2}{Z_1}\cdot\left(\frac{\delta T_c}{\delta R}\cdot \overline{T_c} + T_c \cdot \overline{\left(\frac{\delta T_c}{\delta R}\right)}\right)$$

EQN 4- 17

The partial derivative of the transmission coefficient and the reflection coefficient require that the partial derivative of the transfer matrix with respect to R be obtained. This analysis is described in Appendix B and is based upon the work of Li [1]. The analysis provides expressions for the two partial derivatives:

$$\frac{\delta R_c}{\delta R} = \frac{2\cdot Z_1 \cdot \left[\omega^2\cdot Z_2 \cdot \left(t_{12}(R)\cdot t_{21\_prime}(R) - t_{12\_prime}(R)\cdot t_{21}(R) + t_{11\_prime}(R)\cdot t_{22}(R) - t_{11}(R)\cdot t_{22\_prime}(R)\right)\cdots \atop +j\cdot\left[\omega^3\cdot Z_2^2\cdot\left(t_{11\_prime}(R)\cdot t_{12}(R) - t_{11}(R)\cdot t_{12\_prime}(R)\right) - \omega\cdot\left(t_{21\_prime}(R)\cdot t_{22}(R) - t_{21}(R)\cdot t_{22\_prime}(R)\right)\right]\right]}{\left[\left(t_{21}(R) - \omega^2\cdot Z_1\cdot Z_2\cdot t_{12}(R)\right) + j\cdot\omega\cdot\left(t_{22}(R)\cdot Z_1 + t_{11}(R)\cdot Z_2\right)\right]^2}$$

EQN 4- 18

and:

$$\frac{\delta T_c}{\delta R} = 2 \cdot Z_1 \cdot \left[\frac{\omega^2 \cdot \left(t_{22\_prime}(R) \cdot Z_1 + t_{11\_prime}(R) \cdot Z_2\right) + j \cdot \left(\omega^3 \cdot Z_1 \cdot Z_2 \cdot t_{12\_prime}(R) - \omega \cdot t_{21\_prime}(R)\right)}{\left[\left(t_{21}(R) - \omega^2 \cdot Z_1 \cdot Z_2 \cdot t_{12}(R)\right) + j \cdot \omega \cdot \left(t_{22}(R) \cdot Z_1 + t_{11}(R) \cdot Z_2\right)\right]^2} \right]$$

<div align="right">EQN 4- 19</div>

The determination of the optimum value of the damper to absorb the maximum energy becomes a numerical solution, given the physical characteristics of the mooring system. The extreme case is the replacement of the second mass to encounter the incoming wave in Figure 4-1(M_2) with a hinge termination. The optimum value of the damper would be when the damper impedance was equal to the impedance of the input cable:

$$R_{optimum} = \rho c \frac{L^2}{b^2} \quad \text{therefore: Damper Ratio} = \frac{R}{R_{optimum}} \quad \text{or Damper Ratio} = \frac{Rb^2}{\rho cL^2}$$

<div align="right">EQN 4- 20</div>

Where R is the value of the damper, b is the transverse distance from the centerline of the system to the location of the damper, L is the length of the first mass (h in Figure 4-1), ρ is the linear density of the cable, and c is the speed of the wave traveling along the cable. A comparison with the value of this optimum damper will provide a great deal of insight on the performance of the evaluation and design process.

The design process described in Appendix B was based upon the fact that the user will know the value of the linear density of the cable and the range of tension expected in the system. From these two parameters, the impedance of the cables (Z_1 and Z_2 in Figure 4-1) can be easily determined. Using those impedances as the entry point in the design process, a new set of resonance frequencies must be obtained using the process described in Appendix A. Based upon the highest of the two frequencies calculated, the optimum value of the damper is numerically determined using the secant method for the derivative

by substituting equations 4-19 and 4-18 into equation 4-17. This process is done over a range of values for the cable impedance, and the results are
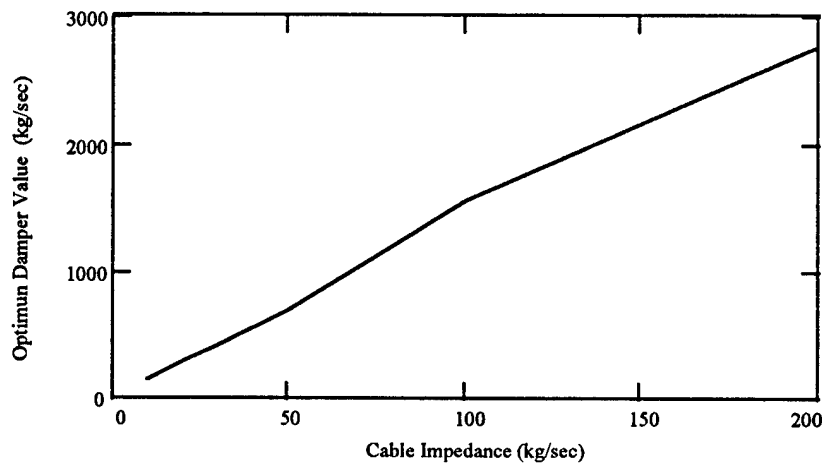

Figure 4- 4: Plot of Optimum Damper Value versus Cable Impedance Using Input Parameters from Table 4-1 and Evaluated at the Corresponding Ω_2

plotted in Figure 4-4. The range of the cable impedance varied from 10 to 200 kg/sec, maintaining the value of the linear density of the cable constant. The linear density as well as the rest of the physical characteristics are the same as the values as outlined in Table 4-1, with the exception of the tension at T_i and T_{i-1} which must be altered in order to maintain the desired value for the cable impedance maintaining the linear density of the cable constant.

A plot of the values of the absorption power ratio versus the damper values for varying increments of the cable impedance is provided in Figure 4-5. When the damper values are divided by the cable impedance for the particular variant ($Z_1=Z_2=Zc$), the curves closely follow each other, with a maximum absorption power ratio of approximately .5 at a damper ratio of approximately .11. This is shown in Figure 4-6. The variance of the cable impedance does not have a drastic affect on the maximum absorption power ratio.

The variation of the optimum damper is also affected by the mass of the component masses M_1 and M_2. With the other physical characteristics held constant, the

28
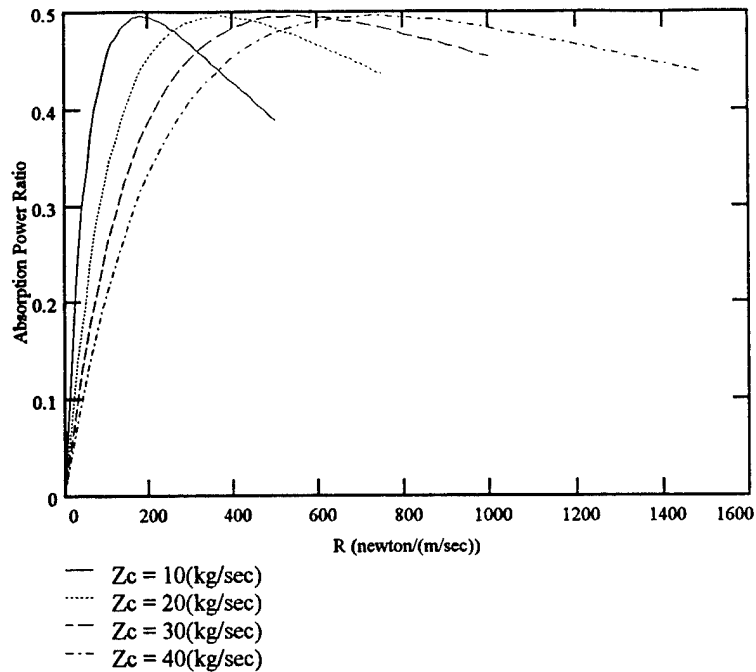
Figure 4- 5: Plot of Absorption Power Ratio for Varying Input Impedances Using Input Parameters from Table 4-1 and Evaluated at the Corresponding Ω_2
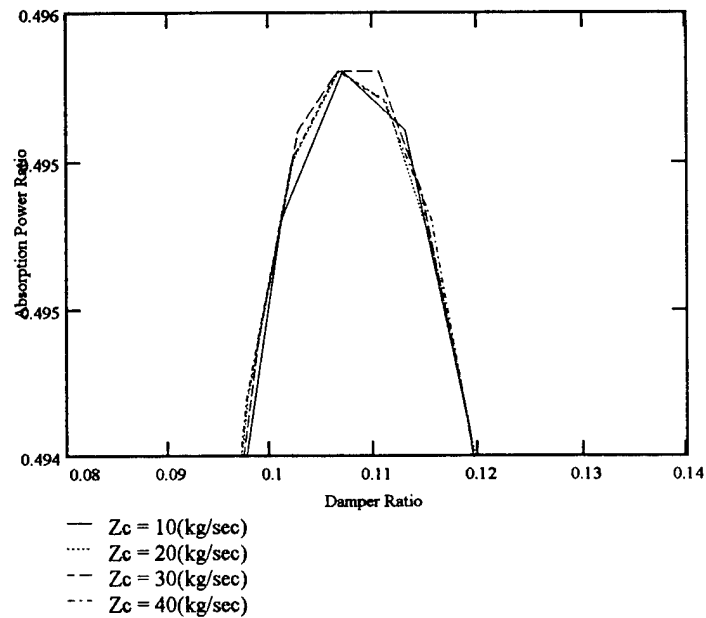
Figure 4- 6: Plot of Absorption Power Ratio Using Input Parameters from Table 4-1 and Evaluated at the Corresponding Ω_2 for Varying Input Impedances
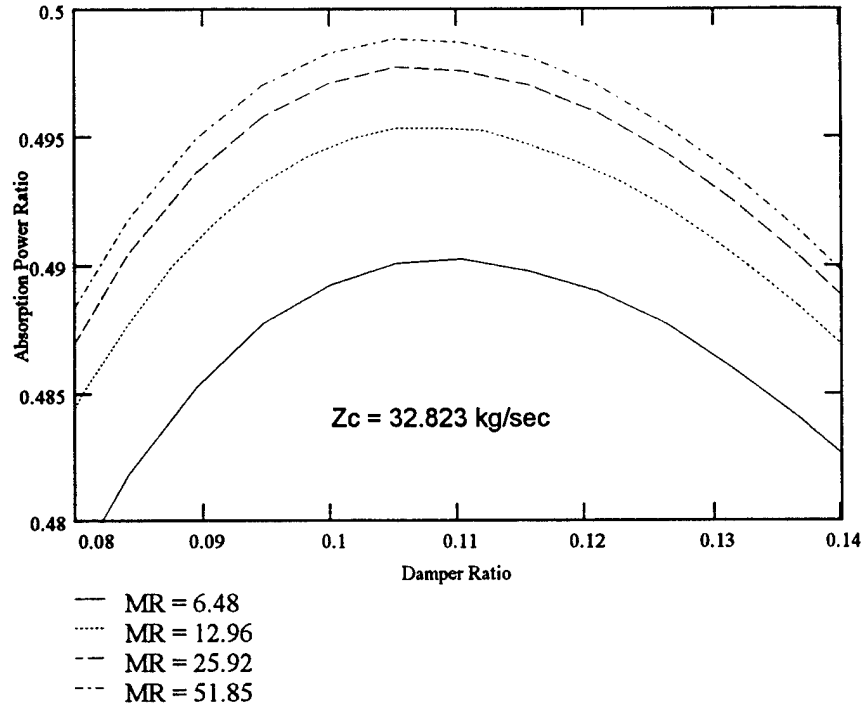
Figure 4- 7: Plot of Absorption Power Ratio for Varying Mass Ratios ($M_1=M_2$) Using Input Parameters from Table 4-1 and Evaluated at the Corresponding Ω_2

change in the optimum value of the damper with the varying values of the masses($M_1=M_2$) is shown in Figure 4-7. Here the mass of the two components is compared to the mass of an equivalent length of cable. The mass ratio is defined by:

$$MR = \frac{M_1 + M_2}{2\rho_1 d + 2\rho_2 f}$$

EQN 4- 21

Note that the increase in mass tends to increase the absorption power ratio, and it asymptotically approaches a maximum value of .5 when both masses are increased the same amount. If the two masses are not altered equally, varying the mass ratio will alter the absorption power ratio differently. Figure 4-8 shows that an increase in the mass of M_1 while maintaining M_2 constant tends to decrease the value of the absorption power
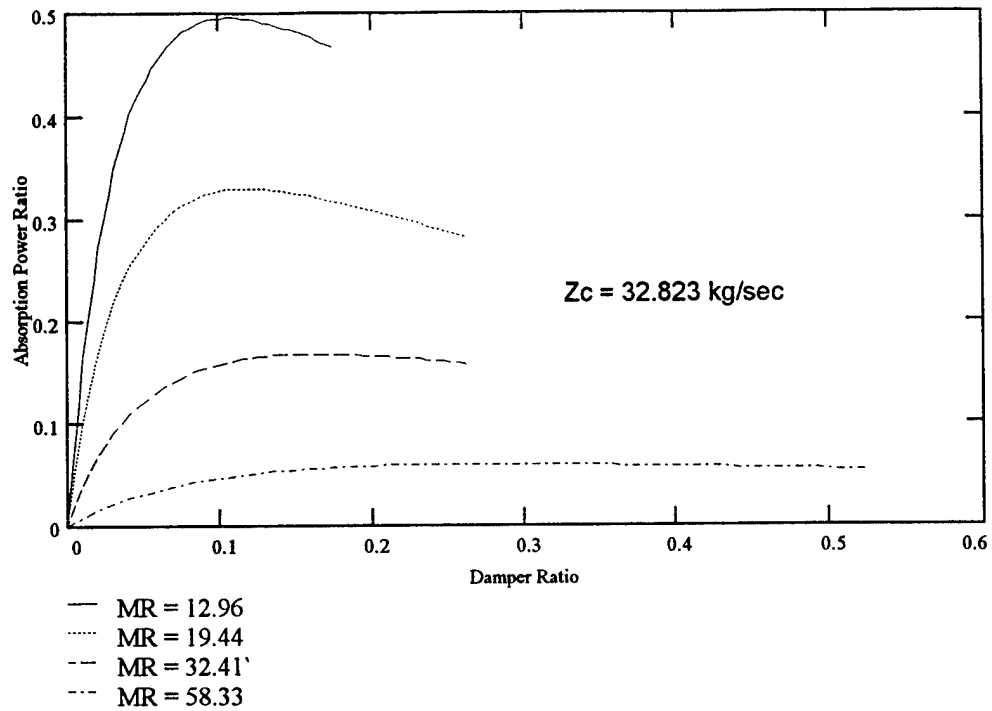
Figure 4- 8: Plot of Absorption Power Ratio Varying Mass Ratios (Alter M_1 only) Using Input Parameters from Table 4-1 and Evaluated at the Corresponding Ω_2

Figure 4- 9: Plot of Absorption Power Ratio Varying Mass Ratios (Alter M_2 only) Using Input Parameters from Table 4-1 and Evaluated at the Corresponding Ω_2
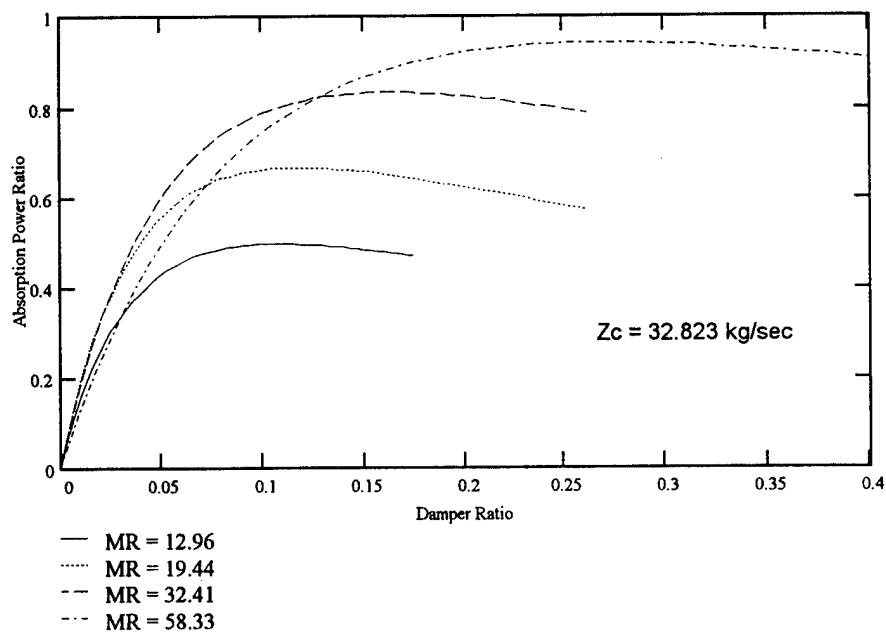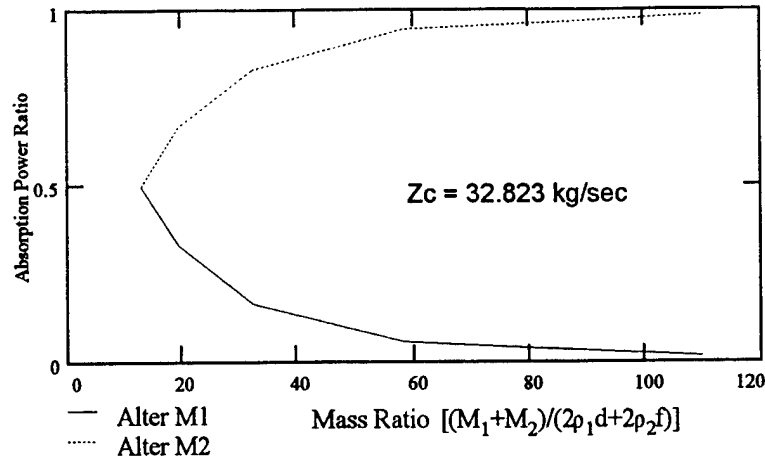
31

Zc = 32.823 kg/sec

— Alter M1   Mass Ratio $[(M_1+M_2)/(2\rho_1 d+2\rho_2 f)]$
⋯⋯ Alter M2

Figure 4- 10: Plot of Absorption Power Ratio varying Mass Ratio (Alter M_1 or M_2 only) Using Input Parameters from Table 4-1 and Evaluated at the Corresponding Ω_2

ratio, while Figure 4-9 shows that an increase in the mass of M_2 while maintaining M_1 constant tends to increase the value of the absorption power ratio. Figure 4-10 shows the trend towards reaching the ultimate value of total absorption at the second resonance frequency as the mass ratio of the system is increased by altering the mass ratio with increasing M_1 or M_2 only.

Another physical characteristic of the system involves the lengths of the components. If the lengths of the components are changed, the natural frequencies and the corresponding values of the optimum damper will also change. Figure 4-11 represents the effect that changing the length of M_1 and M_2 has on the performance of the system, using the following relationship for the length ratio:

$$LR = \frac{d}{f}$$ EQN 4- 22

Where d and f are the lengths described in Figure 4-1. Note that the location of the center peak for the value of the damper in Figure 4-11 is not constant for the five different length variations as it was for the mass and the impedance variants. An increase in the length of M_1 while keeping the length of M_2 constant causes a decrease in the absorption power ratio, whereas the increase in length of M_2 while keeping M_1 constant increases the

32
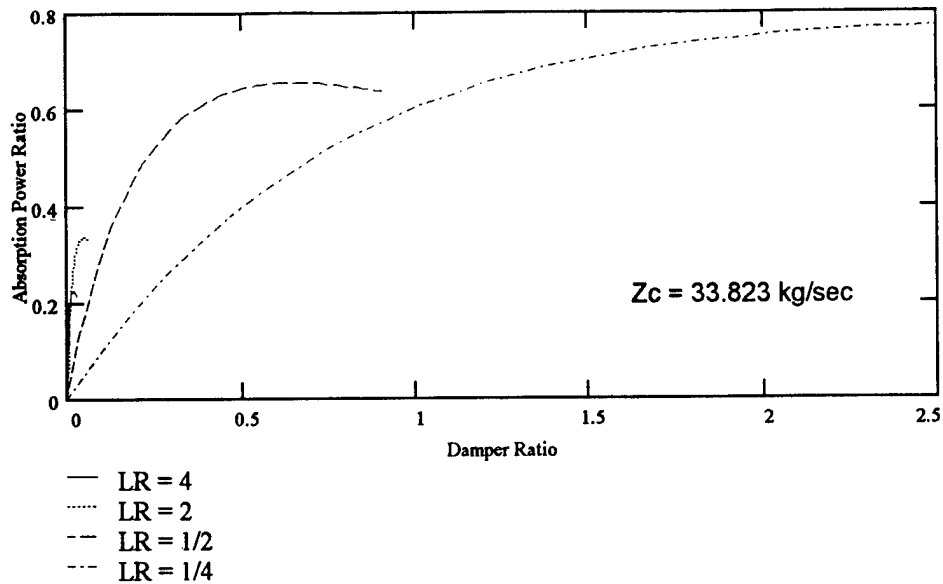
Figure 4- 11: Plot of Absorption Power Ratio Varying Length Ratio Using Input Parameters from Table 4-1 and Evaluated at the Corresponding Ω_2

absorption power ratio. The geometry of the system is the dominant term in determining the location of this peak value. While altering the length, the other constants outlined in Table 4-1 remained constant with the exception of the moment of inertia which is affected by the geometrical changes.

The common factor in both the mass and the length analysis is that an increase in the moment of inertia in the first mass to see the incoming wave as defined by the analysis (M_1), whether caused by an increase of mass or a geometrical change, decreases the absorption power ratio, and less energy is absorbed in the system. An increase in the moment of inertia of the second mass in the system to see the wave (M_2), will correspondingly increase the absorption power ratio and improve the system performance if the location of the external force can be identified.

Even though the lower resonance frequency provides a location when the reflection coefficient is zero, the system does not have enough relative motion between the two masses to absorb a great deal of energy. This is shown in Figure 4-12.
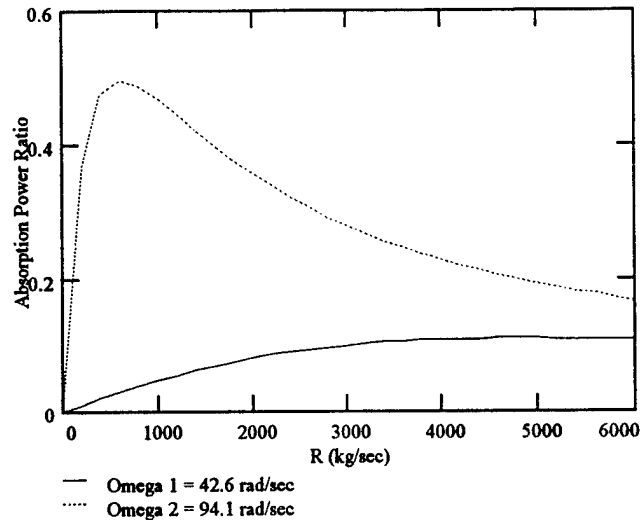
Figure 4- 12: Comparison of Absorption Power Ratios for the Two Resonance Frequencies Using Input Parameters from Table 4-1

The complexities of the algebra involved with the formulation of the design tools could lead to an error that is not readily noticeable. An attempt was made to validate the results of this analysis with an independent source. Hayner [7] used a spectral finite element method to calculate transmission power, absorption, and reflection in cable systems. Similar to conventional finite element methods, a stiffness matrix is formulated, which relates the element displacements to the applied forces at nodes due to either other elements or external forces. The stiffness matrix includes mass and dissipative effects, as well, by letting the matrix elements be complex. Formulating the cable dynamics in terms of a stiffness matrix brings to bear well known finite element solution procedures discussed by Bathe [8] for solving the response of interconnected elements. The spectral finite element differs from a conventional finite element in that the formulation is based on a wave solution, which is exact to within the assumptions inherent in the governing differential equation. Two additional matrices relating element displacements to wave amplitudes and forces to wave amplitudes are used to calculate reflection, transmission, and absorption coefficients. The spectral finite element approach may also be considered a generalization of the transfer matrix approach discussed by Fertis [9].

34
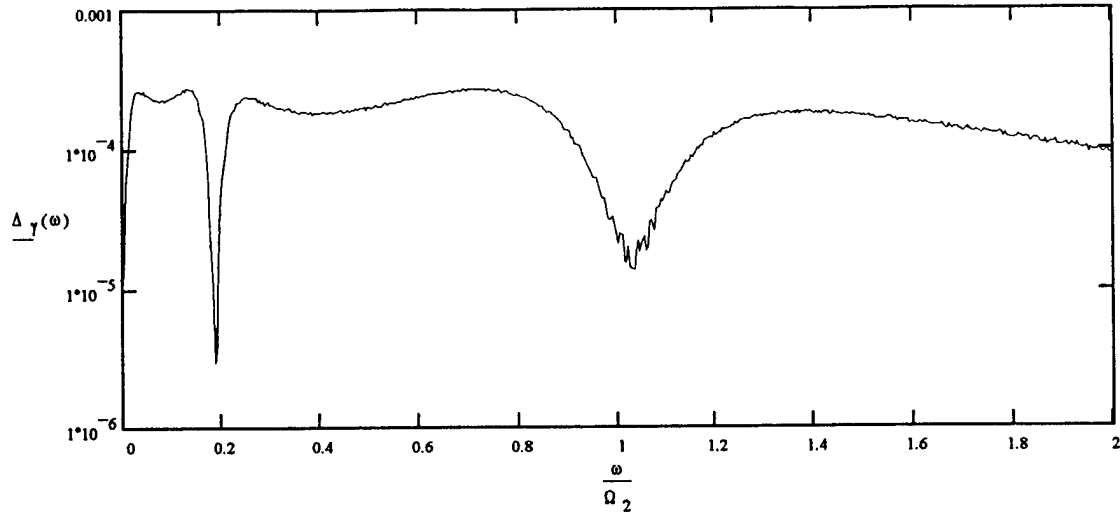
Figure 4- 13: Error Comparison with Hayner Method of Transmission Power Ratio Using Input Parameters from Table 4-1 and R= 20 kg/sec and $I_1=I_2=.005$ kgm^2

A comparison of the two methods is provided in Figure 4-13 and 4-14. The input data is provided in Table 4-1 with the exception that the value for the damper is set at 20
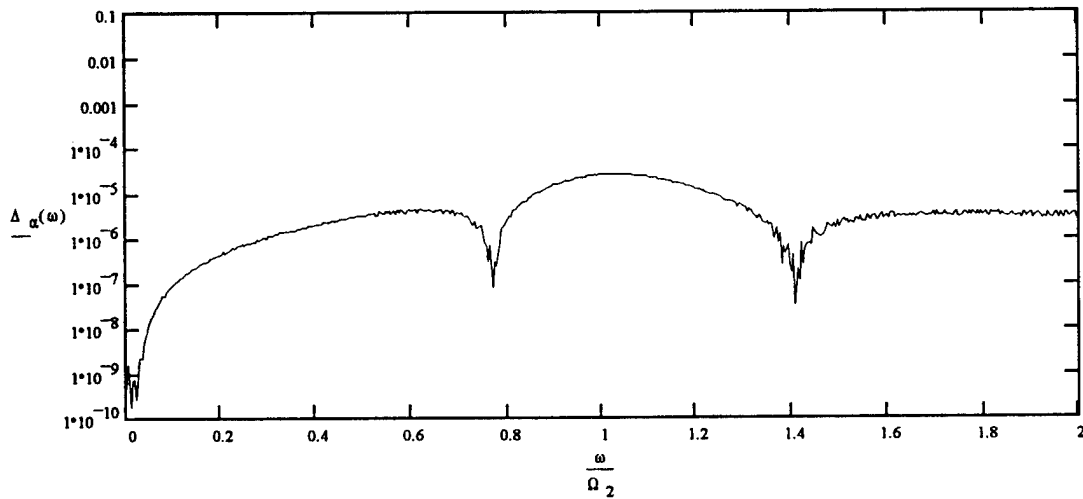
Figure 4- 14: Error Comparison with Hayner Method of Absorption Power Ratio Using Input Parameters from Table 4-1 and R= 20 kg/sec and $I_1=I_2=.005$ kgm^2

kg/sec and the moment of inertia of the two masses ($I_1 = I_2$) is .005 kg m^2. Figure 4-13 is the absolute value of the difference in the transmission power ratios for the two methods. Figure 4-14 is the absolute value of the difference in the absorption power ratio between the two methods. Both comparisons reveal that the two methods provide nearly identical results for both the absorption power ratio and the transmission power ratio

Chapter 5

Final Results/ Recommendations for Further Research

The analysis of the moored cable system with the in-line absorber was very effective. For varying values of cable impedance, an optimum value of the damper was determined. Throughout the entire range of the possible forced vibrations considered from vortex induced forces, there was a corresponding value of a damper that could mitigate the effect of the motions. This will allow the tuning of the system to help prevent the lock-in of the response of the cable with a forcing function near its resonant frequency.

Throughout the entire effort to determine the value of the damper that would provide the maximum amount of power absorption, the magnitude of the absorption power ratio was limited to .5 when alterations were made symmetrically with respect to the characteristics of the two masses. This matches well with previous attempts to maximize the energy absorbed in a cable system by Vandiver and Li [10], although that analysis involved the use of a different type of absorber that had three masses instead of two and two springs and two dampers.

When an investigation was performed on the behavior of the system with increased cable impedance while maintaining the linear density constant the results indicated a near linear relationship between the value of the damper required in order to absorb the maximum amount of energy and the tension seen on the cable. As the tension increased, the value of the damper required in order to absorb the maximum amount of power also increased. A second independent researcher, Hayner, was able to duplicate the results obtained in chapter four with a basis of only the input parameters, an indication that the process was correct.

The alterations of the physical characteristics of the masses had a great affect on the behavior of the system as a whole. An increase in mass of the system, if divided equally between the two component masses, did not provide as much absorption as a concentration of the increase in mass in M_2 alone, where an absorption power ratio of nearly 1.0 was obtained when the mass of M_2 was 16 times M_1. The limit to that approach

is that the differences between the two masses would have other second order affects on the system that are not modeled in this analysis. An increase in the mass of M_1 alone decreased the value of the absorption power ratio, decreasing optimum power absorption.

The alteration of the component mass lengths also had a significant effect on the maximum power absorbed. An increase in the length of M_1 decreased the absorption power ratio, and an increase in the length of M_2 increased the absorption power ratio. These trends follow the observations of the mass changes described above. In both instances, the changes reflected changes in the moments of inertia of the component masses. When the moment of inertia of M_2 was increased such that it resembled a fixed pin, the power absorption was increased.

The first area that requires further research is the application of this process to the finite case, where the existence of the boundary conditions at the termination of the system would alter the results of this infinite cable application.

The dynamic response of the system to varying currents or changes in speed should be included in a further study of the system.

The inclusion of the bending stiffness of a cable would provide a more robust model with a more detailed wave propagation.

The construction and testing of a real world absorber would apply the principles of this thesis and validate the power absorption methodology.

Additionally, an investigation should be made into the effects that multiple in-line damper systems will have on the behavior of the system as a whole.

References

1. Li,L. 1993. *The Dynamics of Strings with Rigid Lumps*. PhD. Thesis. Massachusetts Institute of Technology.

2. National Research Council (NRC). 1990. *Managing Troubled Waters*. Washington, D.C. National Academy Press.

3. Kildow, J. T. and M. Lohse. 1995. *Project Report, Stellwagen Bank National Marine Sanctuary Monitoring Plan*. Massachusetts Institute of Technology.

4. Triantafyllou, M. S. and Chryssostomidis, C. 1980. *Environment Description, Force Prediction and Statistics for Design Applications in Ocean Engineering*. Massachusetts Institute of Technology.

5. Meirovitch, L. 1975. *Elements of Vibration Analysis*. McGraw-Hill. New York

6 Vandiver, J. K. 1982. *A Comparison Between Predicted and Measured Natural Frequencies in Water for the Castine Cable with Attached Masses*. Massachusetts Institute of Technology.

7. Hayner, M. 1996. Personal Communication. Massachusetts Institute of Technology.

8. Bathe, K. J. 1988. *Finite Element Procedures in Engineering Analysis*. Prentice-Hall. New Jersey.

9. Fertis, D. G. 1995. *Mechanical and Structural Vibrations*. J. Wiley & Sons, Inc. New York.

10. Vandiver, J. K. Li, L. 1993. *Vibration Suppression of Tension-Dominated Slender Structures By Dynamic Absorbers*. Massachusetts Institute of Technology.

Appendix A

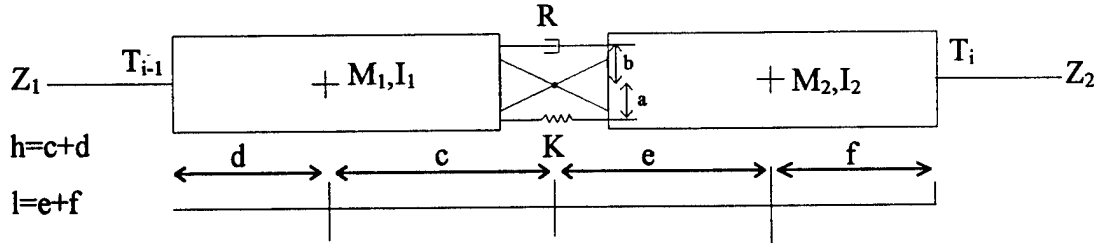## Determination of the Zeros of the Reflection Coefficient

Figure A-1: Schematic of the System

Based upon the formulations of the transfer matrix equations from Li, the following analysis describes the approach to determining the location of the frequencies where the power absorption will be a maximum. A computer program, Mathcad 5.0[®], was used in the calculation process.

The first expressions to determine the transfer matrix are expressed in terms of the values of the particular dimensions:

$$\alpha_1(\omega) := T_{i\_minus} \cdot d + H \cdot c + K \cdot a^2 - (\omega)^2 \cdot I_1 + j \cdot \omega \cdot R \cdot b^2 \qquad \alpha_2(\omega) := T_i \cdot f + H \cdot e + K \cdot a^2 - (\omega)^2 \cdot I_2 + j \cdot \omega \cdot R \cdot b^2$$

$$\alpha_3(\omega) := K \cdot a^2 + j \cdot \omega \cdot R \cdot b^2$$

The Intermediate equations are expressed:

$$\gamma_1(\omega) := \frac{-\left(M_1 \cdot l + M_2 \cdot f\right) \cdot \alpha_1(\omega) - M_1 \cdot c \cdot \left(\alpha_3(\omega)\right) + (\omega)^2 \cdot M_1 \cdot M_2 \cdot f \cdot c^2}{M_2 \cdot c \cdot \left(\alpha_1(\omega)\right) + \left(M_1 \cdot d + M_2 \cdot h\right) \cdot \left(\alpha_3(\omega)\right) + (\omega)^2 \cdot M_1 \cdot M_2 \cdot c \cdot d}$$

$$\gamma_2(\omega) := \frac{-M_2 \cdot f \cdot h^2 - M_1 \cdot l \cdot d^2 + \dfrac{\left[\left(\alpha_1(\omega)\right) \cdot l + \left(\alpha_3(\omega)\right) \cdot h\right]}{(\omega)^2}}{M_2 \cdot c \cdot \left(\alpha_1(\omega)\right) + \left(M_1 \cdot d + M_2 \cdot h\right) \cdot \left(\alpha_3(\omega)\right) + (\omega)^2 \cdot M_1 \cdot M_2 \cdot c \cdot d}$$

$$\gamma_3(\omega) := -\left[\frac{M_1 \cdot d \cdot l \cdot c + \left[\dfrac{\left[\left(\alpha_1(\omega)\right) \cdot l + \left(\alpha_3(\omega)\right) \cdot h\right]}{(\omega)^2}\right]}{M_2 \cdot c \cdot \left(\alpha_1(\omega)\right) + \left(M_1 \cdot d + M_2 \cdot h\right) \cdot \left(\alpha_3(\omega)\right) + (\omega)^2 \cdot M_1 \cdot M_2 \cdot c \cdot d}\right]$$

40

The intermediate expressions continue:

$$\gamma_4(\omega) := -\left[\frac{\left(M_1 \cdot l + M_2 \cdot f\right)\cdot\left(\alpha_3(\omega)\right) + M_1 \cdot e \cdot \alpha_2(\omega) + (\omega)^2 \cdot M_1 \cdot M_2 \cdot e \cdot c \cdot f}{\dfrac{\left(\alpha_2(\omega)\cdot h + \alpha_3(\omega)\cdot l\right)}{\omega^2} - \left(M_1 \cdot d \cdot l^2 + M_2 \cdot f^2 \cdot h\right)}\right]$$

$$\gamma_5(\omega) := \frac{\left[\dfrac{\left(\alpha_2(\omega)\cdot h + \alpha_3(\omega)\cdot l\right)}{\omega^2}\right] + M_2 \cdot e \cdot f \cdot h}{\dfrac{\left(\alpha_2(\omega)\cdot h + \alpha_3(\omega)\cdot l\right)}{\omega^2} - \left(M_1 \cdot d \cdot l^2 + M_2 \cdot f^2 \cdot h\right)}$$

$$\gamma_6(\omega) := \frac{-\alpha_2(\omega)\cdot\left(M_1 \cdot d + M_2 \cdot h\right) - M_2 \cdot e \cdot \alpha_3(\omega) + (\omega)^2 \cdot M_1 \cdot M_2 \cdot e^2 \cdot d}{\dfrac{\left(\alpha_2(\omega)\cdot h + \alpha_3(\omega)\cdot l\right)}{\omega^2} - \left(M_1 \cdot d \cdot l^2 + M_2 \cdot f^2 \cdot h\right)}$$

Now knowing these, the transfer matrix can be determined:

$$t_{11}(\omega) := \gamma_1(\omega) + \gamma_3(\omega)\cdot\frac{\gamma_4(\omega) + \gamma_1(\omega)\cdot\gamma_6(\omega)}{1 - \gamma_3(\omega)\cdot\gamma_6(\omega)} \qquad t_{12}(\omega) := \gamma_2(\omega) + \gamma_3(\omega)\cdot\frac{\gamma_5(\omega) + \gamma_2(\omega)\cdot\gamma_6(\omega)}{1 - \gamma_3(\omega)\cdot\gamma_6(\omega)}$$

$$t_{21}(\omega) := \frac{\gamma_4(\omega) + \gamma_1(\omega)\cdot\gamma_6(\omega)}{1 - \gamma_3(\omega)\cdot\gamma_6(\omega)} \qquad t_{22}(\omega) := \frac{\gamma_5(\omega) + \gamma_2(\omega)\cdot\gamma_6(\omega)}{1 - \gamma_3(\omega)\cdot\gamma_6(\omega)}$$

Now the reflection and transmission coefficients are determined

$$R_c(\omega) := \frac{-\left[\left(t_{21}(\omega)\right) + (\omega)^2 \cdot Z_1 \cdot Z_2 \cdot t_{12}(\omega)\right] + j\cdot\omega\cdot\left(Z_1 \cdot t_{22}(\omega) - Z_2 \cdot t_{11}(\omega)\right)}{t_{21}(\omega) - (\omega)^2 \cdot Z_1 \cdot Z_2 \cdot t_{12}(\omega) + j\cdot\omega\cdot\left(Z_1 \cdot t_{22}(\omega) + Z_2 \cdot t_{11}(\omega)\right)}$$

$$T_c(\omega) := \frac{j\cdot 2\cdot\omega\cdot Z_1}{t_{21}(\omega) - (\omega)^2 \cdot Z_1 \cdot Z_2 \cdot t_{12}(\omega) + j\cdot\omega\cdot\left(Z_1 \cdot t_{22}(\omega) + Z_2 \cdot t_{11}(\omega)\right)}$$

The Power Reflection, Transmission and Absorption Ratios are:

$$\beta(\omega) := R_c(\omega)\cdot\overline{R_c(\omega)} \qquad \gamma(\omega) := \frac{Z_2}{Z_1}\cdot T_c(\omega)\cdot\overline{T_c(\omega)} \qquad \alpha(\omega) := 1 - \beta(\omega) - \gamma(\omega)$$

The input impedance is:

$$Z_m = \frac{force}{velocity} \qquad \text{and} \qquad Z_m(\omega) := \frac{t_{21}(\omega) + j\cdot\omega\cdot Z_2 \cdot t_{11}(\omega)}{-\omega^2 \cdot Z_2 \cdot t_{12}(\omega) + j\cdot\omega\cdot t_{22}(\omega)}$$

41

In order to determine a numerical solution for the analysis, physical characteristics of the system must be input. These values used here and throughout the thesis are based upon a real world oceanographic mooring described by Vandiver, discussed in chapter 4. The following are the physical characteristics of this system:

$a := .0254 \cdot m$ $d := .1524 \cdot m$ $c := .1778 \cdot m$ $h := c + d$ $M_1 := 4.52 \cdot k$ $I_1 := \dfrac{M_1 \cdot (2 \cdot d)^2}{12}$

$b := .0254 \cdot m$ $f := .1524 \cdot m$ $e := .1778 \cdot m$ $l := e +$ $M_2 := 4.52 \cdot k$ $I_2 := \dfrac{M_2 \cdot (2 \cdot f)^2}{12}$

$\rho_1 := 1.144 \cdot \dfrac{kg}{m}$ $\rho_2 := 1.144 \cdot \dfrac{kg}{m}$ $Z_1 := 33.8231 \cdot \dfrac{kg}{sec}$ $Z_2 := 33.8231 \cdot \dfrac{kg}{sec}$ $K := 10 \cdot \dfrac{newton}{m}$ $R := 0 \cdot \dfrac{newton}{\frac{m}{sec}}$

$H := 1000 \cdot newton$ $T_{i\_minus} := \dfrac{Z_1^2}{\rho_1}$ $T_i := \dfrac{Z_2^2}{\rho_2}$

A curve of the Power and Transmission Coefficients provides an indication where to search for the Resonance Frequencies of the system
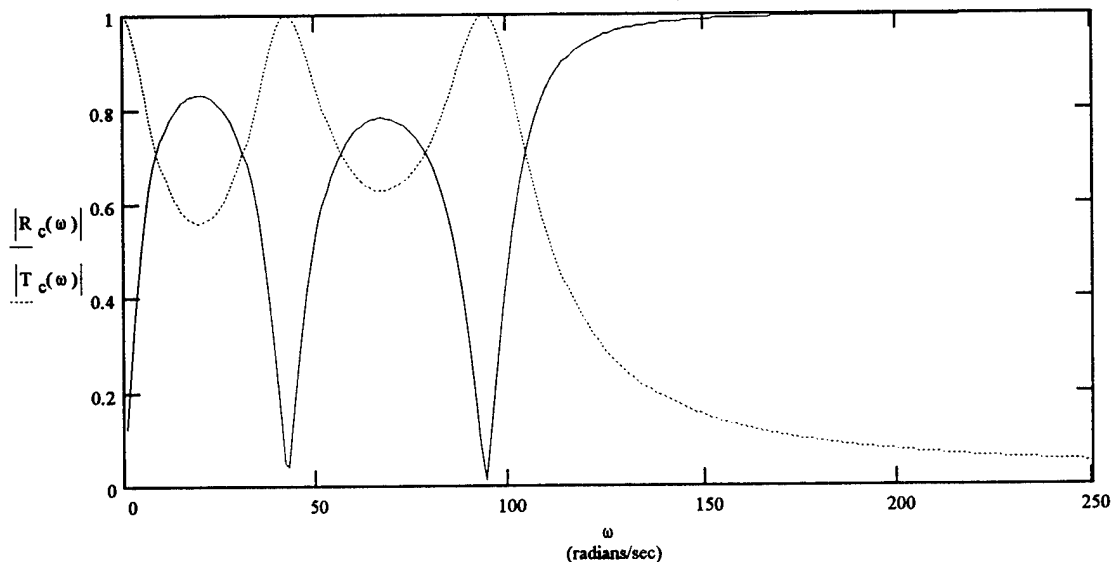
Figure A-2: Graph of Reflection and Transmission Coefficients Using Input Parameters from Table 4-1 (R=0)

Based upon this, it appears as if the best absorption would occur at the frequencies at the location of zeros of the Power Reflection Coefficient. Using the secant method, we

try to obtain these values at the location of the curves where the Power Reflection Coefficient appears to go to zero.

The reflection coefficient can be reduced to:

$$Rc(\omega) = \frac{\left(-t_{21}(\omega)^2 + \omega^4 \cdot Z_1^2 \cdot Z_2^2 \cdot t_{12}(\omega)^2 + \omega^2 \cdot Z_1^2 \cdot t_{22}(\omega)^2 - \omega^2 \cdot Z_2^2 \cdot t_{11}(\omega)^2 + 2i \cdot \omega \cdot Z_1 \cdot t_{22}(\omega) \cdot t_{21}(\omega) + 2i \cdot \omega^3 \cdot Z_1 \cdot Z_2^2 \cdot t_{11}(\omega) \cdot t_{12}(\omega)\right)}{\left(t_{21}(\omega)^2 - 2 t_{21}(\omega) \cdot \omega^2 \cdot Z_1 \cdot Z_2 \cdot t_{12}(\omega) + \omega^4 \cdot Z_1^2 \cdot Z_2^2 \cdot t_{12}(\omega)^2 + \omega^2 \cdot Z_1^2 \cdot t_{22}(\omega)^2 + 2 \cdot \omega^2 \cdot Z_1 \cdot t_{22}(\omega) \cdot Z_2 \cdot t_{11}(\omega) + \omega^2 \cdot Z_2^2 \cdot t_{11}(\omega)^2\right)}$$

And to determine the zeros, we solve for the values of w such that the numerator goes to zero using the secant method.

The first data point is close to 40 rad/sec for the initial guess $\omega := 42.564 \cdot \frac{rad}{sec}$

The expression for the solution is provided:

$$\Omega_{1\_Rc} := \left| root\left[\left(-t_{21}(\omega)^2 + \omega^4 \cdot Z_1^2 \cdot Z_2^2 \cdot t_{12}(\omega)^2 + \omega^2 \cdot Z_1^2 \cdot t_{22}(\omega)^2 - \omega^2 \cdot Z_2^2 \cdot t_{11}(\omega)^2\right) + 2i \cdot \omega \cdot Z_1 \cdot t_{22}(\omega) \cdot t_{21}(\omega) \ldots, \omega \right] \right|$$
$$+ 2i \cdot \omega^3 \cdot Z_1 \cdot Z_2^2 \cdot t_{11}(\omega) \cdot t_{12}(\omega)$$

The resulting resonance frequency is: $\omega := 42.564 \cdot \frac{rad}{sec}$

This convergence represents an iteration between estimate and calculation until the solution converged to the third decimal point.

The second data point is close to 90 rad/sec for the initial guess $\omega := 94.13 \cdot \frac{rad}{sec}$

The expression for the solution is provided:

$$\Omega_{2\_Rc} := \left| root\left[\left(-t_{21}(\omega)^2 + \omega^4 \cdot Z_1^2 \cdot Z_2^2 \cdot t_{12}(\omega)^2 + \omega^2 \cdot Z_1^2 \cdot t_{22}(\omega)^2 - \omega^2 \cdot Z_2^2 \cdot t_{11}(\omega)^2\right) + 2i \cdot \omega \cdot Z_1 \cdot t_{22}(\omega) \cdot t_{21}(\omega) \ldots, \omega \right] \right|$$
$$+ 2i \cdot \omega^3 \cdot Z_1 \cdot Z_2^2 \cdot t_{11}(\omega) \cdot t_{12}(\omega)$$

The resulting resonance frequency is: $\omega := 94.13 \cdot \frac{rad}{sec}$

This convergence represents an iteration between estimate and calculation until the solution converged to the third decimal point.

A second determination of the natural frequencies relies on the determination of the value of w when the input impedance matches that of the input string. Because the string has a purely real impedance, the value of ω such that the imaginary part of the input impedance is zero will provide this frequency.

The imaginary part of the input impedance is described by:

$$Z_m \text{ (imaginary)} = \frac{-\omega^3 \cdot Z_2{}^2 \cdot t_{11}(\omega) \cdot t_{12}(\omega) - t_{21}(\omega) \cdot \omega \cdot t_{22}(\omega)}{\omega^4 \cdot Z_2{}^2 \cdot t_{12}(\omega)^2 + \omega^2 \cdot t_{22}(\omega)^2}$$

Again, the basis for the determinations of the value of ω such that the expression is zero is the location of the minimum values of the Reflection coefficient observed from the graph, and using the secant method, we can determine the resonance frequencies.

The first data point is close to 40 rad/sec: $\omega := 42.564 \cdot \frac{rad}{sec}$

The expression for the solution is provided:

$$\Omega_{1\_Zm} := \text{root}\left(-\omega^3 \cdot Z_2{}^2 \cdot t_{11}(\omega) \cdot t_{12}(\omega) - t_{21}(\omega) \cdot \omega \cdot t_{22}(\omega), \omega\right)$$

The resulting resonance frequency is: $\omega := 42.564 \cdot \frac{rad}{sec}$

This convergence represents an iteration between estimate and calculation until the solution converged to the third decimal point.

The second value appears to be around 90 rad/sec $\omega := 94.13 \cdot \frac{rad}{sec}$

The expression for the solution is provided:

$$\Omega_{2\_Zm} := \text{root}\left(-\omega^3 \cdot Z_2{}^2 \cdot t_{11}(\omega) \cdot t_{12}(\omega) - t_{21}(\omega) \cdot \omega \cdot t_{22}(\omega), \omega\right)$$

The resulting resonance frequency is: $\omega := 94.13 \cdot \frac{rad}{sec}$

This convergence represents an iteration between guess and calculation until the solution converged to the third decimal point. For the impedance method, the result was not as sensitive to the initial estimate of the value of the frequency, but the Reflection Coefficient and the Impedance Method provided the same results.

A sketch of the two mode shapes that correspond to the location of the reflection zeros are provided in Figure A-3. The sketch represents an estimate of how the two mode shapes can be visualized, although a solution to the total system motions was not performed in order to provide this sketch. Position A and position B are the two extremes of the mode shapes. The slight relative rotation between the two masses in mode 1 represents the amount of absorption that occurs in this mode shape. The extreme relative rotation between the two masses in mode 2 represent the maximum amount of absorption that can take place in the system at the second resonance frequency.
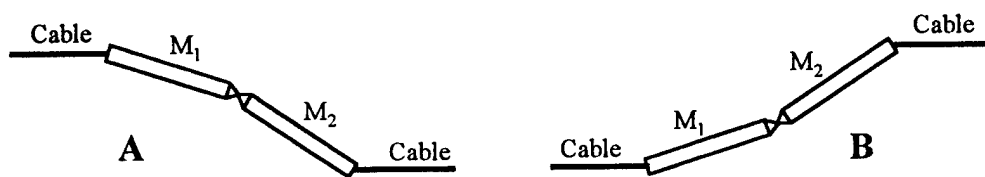
Mode 1: Slight Absorption

Mode 2: Maximum Absorption

Figure A-3: Mode Shape Sketch of System

Appendix B

Determination of the Optimum Damper Values

Based upon the formulations of the transfer matrix equations from Li, the following analysis describes the approach to determining the optimal value of the damper operating at the second resonance frequency. A computer program, Mathcad 5.0®, was used in the calculation process. The first difference between this formulation and Appendix A is the fact that the relationships are dependent upon R, not ω.

$$\alpha_1(R) := T_{i\_minus} \cdot d + H \cdot c + K \cdot a^2 - (\omega)^2 \cdot I_1 + j \cdot \omega \cdot R \cdot b^2 \qquad \alpha_2(R) := T_i \cdot f + H \cdot c + K \cdot a^2 - (\omega)^2 \cdot I_2 + j \cdot \omega \cdot R \cdot b^2$$

$$\alpha_3(R) := K \cdot a^2 + j \cdot \omega \cdot R \cdot b^2$$

Intermediate expressions are described:

$$\gamma_1(R) := \frac{-\left(M_1 \cdot l + M_2 \cdot f\right) \cdot \alpha_1(R) - M_1 \cdot c \cdot \left(\alpha_3(R)\right) + \omega^2 \cdot M_1 \cdot M_2 \cdot f \cdot c^2}{M_2 \cdot c \cdot \left(\alpha_1(R)\right) + \left(M_1 \cdot d + M_2 \cdot h\right) \cdot \left(\alpha_3(R)\right) + \omega^2 \cdot M_1 \cdot M_2 \cdot c \cdot c \cdot d}$$

$$\gamma_2(R) := \frac{-M_2 \cdot f \cdot h^2 - M_1 \cdot l \cdot d^2 + \dfrac{\left[\left(\alpha_1(R)\right) \cdot l + \left(\alpha_3(R)\right) \cdot h\right]}{\omega^2}}{M_2 \cdot c \cdot \left(\alpha_1(R)\right) + \left(M_1 \cdot d + M_2 \cdot h\right) \cdot \left(\alpha_3(R)\right) + \omega^2 \cdot M_1 \cdot M_2 \cdot c \cdot c \cdot d}$$

$$\gamma_3(R) := -\left[\frac{M_1 \cdot d \cdot l \cdot c + \left[\dfrac{\left[\left(\alpha_1(R)\right) \cdot l + \left(\alpha_3(R)\right) \cdot h\right]}{\omega^2}\right]}{M_2 \cdot c \cdot \left(\alpha_1(R)\right) + \left(M_1 \cdot d + M_2 \cdot h\right) \cdot \left(\alpha_3(R)\right) + \omega^2 \cdot M_1 \cdot M_2 \cdot c \cdot c \cdot d}\right]$$

$$\gamma_4(R) := -\left[\frac{\left(M_1 \cdot l + M_2 \cdot f\right) \cdot \left(\alpha_3(R)\right) + M_1 \cdot c \cdot \alpha_2(R) + \omega^2 \cdot M_1 \cdot M_2 \cdot c \cdot c \cdot f}{\dfrac{\left(\alpha_2(R) \cdot h + \alpha_3(R) \cdot l\right)}{\omega^2} - \left(M_1 \cdot d \cdot l^2 + M_2 \cdot f^2 \cdot h\right)}\right]$$

The intermediate expressions continue:

$$\gamma_5(R) := \frac{\left[\dfrac{\left(\alpha_2(R)\cdot h + \alpha_3(R)\cdot l\right)}{\omega^2}\right] + M_2\cdot e\cdot f\cdot h}{\dfrac{\left(\alpha_2(R)\cdot h + \alpha_3(R)\cdot l\right)}{\omega^2} - \left(M_1\cdot d\cdot l^2 + M_2\cdot f^2\cdot h\right)}$$

$$\gamma_6(R) := \frac{-\alpha_2(R)\cdot\left(M_1\cdot d + M_2\cdot h\right) - M_2\cdot e\cdot\alpha_3(R) + \omega^2\cdot M_1\cdot M_2\cdot e^2\cdot d}{\dfrac{\left(\alpha_2(R)\cdot h + \alpha_3(R)\cdot l\right)}{\omega^2} - \left(M_1\cdot d\cdot l^2 + M_2\cdot f^2\cdot h\right)}$$

Now knowing these, the transfer matrix can be determined:

$$t_{12}(R) := \gamma_2(R) + \gamma_3(R)\cdot\frac{\gamma_5(R) + \gamma_2(R)\cdot\gamma_6(R)}{1 - \gamma_3(R)\cdot\gamma_6(R)} \qquad t_{11}(R) := \gamma_1(R) + \gamma_3(R)\cdot\frac{\gamma_4(R) + \gamma_1(R)\cdot\gamma_6(R)}{1 - \gamma_3(R)\cdot\gamma_6(R)}$$

$$t_{21}(R) := \frac{\gamma_4(R) + \gamma_1(R)\cdot\gamma_6(R)}{1 - \gamma_3(R)\cdot\gamma_6(R)} \qquad t_{22}(R) := \frac{\gamma_5(R) + \gamma_2(R)\cdot\gamma_6(R)}{1 - \gamma_3(R)\cdot\gamma_6(R)}$$

Now the reflection coefficient is determined

$$R_c(R) := \frac{-\left[\left(t_{21}(R)\right) + \omega^2\cdot Z_1\cdot Z_2\cdot t_{12}(R)\right] + j\cdot\omega\cdot\left(Z_1\cdot t_{22}(R) - Z_2\cdot t_{11}(R)\right)}{t_{21}(R) - \omega^2\cdot Z_1\cdot Z_2\cdot t_{12}(R) + j\cdot\omega\cdot\left(Z_1\cdot t_{22}(R) + Z_2\cdot t_{11}(R)\right)}$$

The transmission coefficient is determined:

$$T_c(R) := \frac{j\cdot 2\cdot\omega\cdot Z_1}{t_{21}(R) - \omega^2\cdot Z_1\cdot Z_2\cdot t_{12}(R) + j\cdot\omega\cdot\left(Z_1\cdot t_{22}(R) + Z_2\cdot t_{11}(R)\right)}$$

The impedance is:

$$Z_m(R) := \frac{t_{21}(R) + j\cdot\omega\cdot Z_2\cdot t_{11}(R)}{-\omega^2\cdot Z_2\cdot t_{12}(R) + j\cdot\omega\cdot t_{22}(R)}$$

The Power Reflection, Transmission and Absorption Ratios are calculated

$$\beta(R) := R_c(R)\cdot\overline{R_c(R)} \qquad\qquad \gamma(R) := \frac{Z_2}{Z_1}\cdot T_c(R)\cdot\overline{T_c(R)} \qquad\qquad \alpha(R) := 1 - \beta(R) - \gamma(R)$$

47

Now the determination of the optimum value of the damper value to obtain the most absorption can be done by taking the derivative of the Power Absorption Ratio with respect to R.

$$\frac{\delta\alpha}{\delta R} = -\frac{\delta\beta}{\delta R} - \frac{\delta\gamma}{\delta R} \qquad \text{Because} \qquad \alpha = 1 - \beta - \gamma$$

knowing

$$\beta = R_c \cdot \overline{R} \qquad \gamma = \frac{Z_2}{Z_1} \cdot T_c \cdot \overline{T} \qquad \text{leads to:} \qquad \frac{\delta\alpha}{\delta R} = \frac{-\delta\left(R_c \cdot \overline{R_c}\right)}{\delta R} - \frac{\delta\left(\frac{Z_2}{Z_1} \cdot T_c \cdot \overline{T}_c\right)}{\delta R}$$

or

$$\frac{\delta\alpha}{\delta R} = -\left(\frac{\delta R_c}{\delta R} \cdot \overline{R}_c + R_c \cdot \frac{\overline{\delta R_c}}{\delta R}\right) - \frac{Z_2}{Z_1} \cdot \left(\frac{\delta T_c}{\delta R} \cdot \overline{T}_c + T_c \cdot \frac{\overline{\delta T_c}}{\delta R}\right)$$

This derivative requires the calculation of the derivative of the transfer matrix from the constituent components of the system. The intermediate equations are provided.

$$\gamma_{1\_prime\_a}(R) := \left[M_1 \cdot (1+c) + M_2 \cdot f\right] \cdot \left[M_2 \cdot e \cdot \left(\alpha_1(R)\right) + \left(M_1 \cdot d + M_2 \cdot h\right) \cdot \left(\alpha_3(R)\right) + \omega^2 \cdot M_1 \cdot M_2 \cdot c \cdot e \cdot d\right]$$

$$\gamma_{1\_prime\_b}(R) := \left[M_1 \cdot d + M_2 \cdot (e+h)\right] \cdot \left[-\left(M_1 \cdot 1 + M_2 \cdot f\right) \cdot \alpha_1(R) - M_1 \cdot c \cdot \left(\alpha_3(R)\right) + \omega^2 \cdot M_1 \cdot M_2 \cdot f \cdot c^2\right]$$

$$\gamma_{1\_prime}(R) := \frac{j \cdot \omega \cdot b^2 \cdot \left(\gamma_{1\_prime\_a}(R) + \gamma_{1\_prime\_b}(R)\right)}{\left[M_2 \cdot e \cdot \left(\alpha_1(R)\right) + \left(M_1 \cdot d + M_2 \cdot h\right) \cdot \left(\alpha_3(R)\right) + \omega^2 \cdot M_1 \cdot M_2 \cdot c \cdot e \cdot d\right]^2}$$

$$\gamma_{2\_prime\_a}(R) := -\left(\frac{1+h}{\omega^2}\right) \cdot \left[M_2 \cdot e \cdot \left(\alpha_1(R)\right) + \left(M_1 \cdot d + M_2 \cdot h\right) \cdot \left(\alpha_3(R)\right) + \omega^2 \cdot M_1 \cdot M_2 \cdot c \cdot e \cdot d\right]$$

$$\gamma_{2\_prime\_b}(R) := \left[M_1 \cdot d + M_2 \cdot (e+h)\right] \cdot \left[-M_2 \cdot f \cdot h^2 - M_1 \cdot 1 \cdot d^2 + \frac{\left[\left(\alpha_1(R)\right) \cdot 1 + \left(\alpha_3(R)\right) \cdot h\right]}{\omega^2}\right]$$

$$\gamma_{2\_prime}(R) := \frac{j \cdot \omega \cdot b^2 \cdot \left(\gamma_{2\_prime\_a}(R) + \gamma_{2\_prime\_b}(R)\right)}{\left[M_2 \cdot e \cdot \left(\alpha_1(R)\right) + \left(M_1 \cdot d + M_2 \cdot h\right) \cdot \left(\alpha_3(R)\right) + \omega^2 \cdot M_1 \cdot M_2 \cdot c \cdot e \cdot d\right]^2}$$

$$\gamma_{3\_prime\_a}(R) := \left(\frac{1+h}{\omega^2}\right) \cdot \left[M_2 \cdot e \cdot (\alpha_1(R)) + (M_1 \cdot d + M_2 \cdot h) \cdot (\alpha_3(R)) + \omega^2 \cdot M_1 \cdot M_2 \cdot e \cdot d\right]$$

$$\gamma_{3\_prime\_b}(R) := \left[M_1 \cdot d + M_2 \cdot (e+h)\right] \cdot \left[M_1 \cdot d \cdot l \cdot c + \left[\frac{\left[(\alpha_1(R)) \cdot l + (\alpha_3(R)) \cdot h\right]}{\omega^2}\right]\right]$$

$$\gamma_{3\_prime}(R) := \frac{-j \cdot \omega \cdot b^2 \cdot (\gamma_{3\_prime\_a}(R) + \gamma_{3\_prime\_b}(R))}{\left[\left[-M_2 \cdot e \cdot (\alpha_1(R)) - (M_1 \cdot d + M_2 \cdot h) \cdot (\alpha_3(R))\right] - \omega^2 \cdot M_1 \cdot M_2 \cdot e \cdot d\right]^2}$$

$$\gamma_{4\_prime\_a}(R) := \left[-\left[M_1 \cdot (1+c) + M_2 \cdot f\right] \cdot \left[\frac{(\alpha_2(R) \cdot h + \alpha_3(R) \cdot l)}{\omega^2} - \left(M_1 \cdot d \cdot l^2 + M_2 \cdot f^2 \cdot h\right)\right]\right]$$

$$\gamma_{4\_prime\_b}(R) := \left[-\left(\frac{h+l}{\omega^2}\right)\right] \cdot \left[(M_1 \cdot l + M_2 \cdot f) \cdot (\alpha_3(R)) + M_1 \cdot c \cdot \alpha_2(R) + \omega^2 \cdot M_1 \cdot M_2 \cdot e \cdot c \cdot f\right]$$

$$\gamma_{4\_prime}(R) := \frac{-j \cdot \omega \cdot b^2 \cdot (\gamma_{4\_prime\_a}(R) + \gamma_{4\_prime\_b}(R))}{\left[\frac{(\alpha_2(R) \cdot h + \alpha_3(R) \cdot l)}{\omega^2} - \left(M_1 \cdot d \cdot l^2 + M_2 \cdot f^2 \cdot h\right)\right]^2}$$

$$\gamma_{5\_prime}(R) := \frac{j \cdot \omega \cdot b^2 \cdot \left[\frac{h+l}{\omega^2} \cdot \left[\frac{(\alpha_2(R) \cdot h + \alpha_3(R) \cdot l)}{\omega^2} - \left(M_1 \cdot d \cdot l^2 + M_2 \cdot f^2 \cdot h\right) - \left[\left[\frac{(\alpha_2(R) \cdot h + \alpha_3(R) \cdot l)}{\omega^2}\right] + M_2 \cdot e \cdot f \cdot h\right]\right]\right]}{\left[\frac{(\alpha_2(R) \cdot h + \alpha_3(R) \cdot l)}{\omega^2} - \left(M_1 \cdot d \cdot l^2 + M_2 \cdot f^2 \cdot h\right)\right]^2}$$

$$\gamma_{6\_prime\_a}(R) := \left[-\left[M_1 \cdot d + M_2 \cdot (e+h)\right] \cdot \left[\frac{(\alpha_2(R) \cdot h + \alpha_3(R) \cdot l)}{\omega^2} - \left(M_1 \cdot d \cdot l^2 + M_2 \cdot f^2 \cdot h\right)\right]\right]$$

$$\gamma_{6\_prime\_b}(R) := \left[-\left(\frac{h+l}{\omega^2}\right)\right] \cdot \left[-\alpha_2(R) \cdot (M_1 \cdot d + M_2 \cdot h) - M_2 \cdot e \cdot \alpha_3(R) + \omega^2 \cdot M_1 \cdot M_2 \cdot e^2 \cdot d\right]$$

$$\gamma_{6\_prime}(R) := \frac{j \cdot \omega \cdot b^2 \cdot (\gamma_{6\_prime\_a}(R) + \gamma_{6\_prime\_b}(R))}{\left[\frac{(\alpha_2(R) \cdot h + \alpha_3(R) \cdot l)}{\omega^2} - \left(M_1 \cdot d \cdot l^2 + M_2 \cdot f^2 \cdot h\right)\right]^2}$$

The elements of the derivative of the transfer matrix are then calculated:

$$t_{21\_prime\_a}(R) := \gamma_{4\_prime}(R) + \gamma_{1\_prime}(R)\cdot\gamma_6(R) + \gamma_1(R)\cdot\gamma_{6\_prime}(R) + \gamma_{3\_prime}(R)\cdot\gamma_4(R)\cdot\gamma_6(R)$$

$$t_{21\_prime\_b}(R) := -\gamma_3(R)\cdot\gamma_{4\_prime}(R)\cdot\gamma_6(R) + \gamma_3(R)\cdot\gamma_4(R)\cdot\gamma_{6\_prime}(R) \cdots$$
$$+ \left(\gamma_1(R)\cdot\gamma_{3\_prime}(R) - \gamma_{1\_prime}(R)\cdot\gamma_3(R)\right)\cdot\left(\gamma_6(R)\right)^2$$

$$t_{21\_prime}(R) := \frac{t_{21\_prime\_a}(R) + t_{21\_prime\_b}(R)}{\left(1 - \gamma_3(R)\cdot\gamma_6(R)\right)^2}$$

$$t_{22\_prime\_a}(R) := \gamma_{5\_prime}(R) + \gamma_{2\_prime}(R)\cdot\gamma_6(R) + \gamma_2(R)\cdot\gamma_{6\_prime}(R) + \gamma_{3\_prime}(R)\cdot\gamma_5(R)\cdot\gamma_6(R)$$

$$t_{22\_prime\_b}(R) := -\gamma_3(R)\cdot\gamma_{5\_prime}(R)\cdot\gamma_6(R) + \gamma_3(R)\cdot\gamma_5(R)\cdot\gamma_{6\_prime}(R) \cdots$$
$$+ \left(\gamma_2(R)\cdot\gamma_{3\_prime}(R) - \gamma_{2\_prime}(R)\cdot\gamma_3(R)\right)\cdot\left(\gamma_6(R)\right)^2$$

$$t_{22\_prime}(R) := \frac{t_{22\_prime\_a}(R) + t_{22\_prime\_b}(R)}{\left(1 - \gamma_3(R)\cdot\gamma_6(R)\right)^2}$$

$$t_{11\_prime}(R) := \gamma_{1\_prime}(R) + \gamma_{3\_prime}(R)\cdot t_{21}(R) + \gamma_3(R)\cdot t_{21\_prime}(R)$$

$$t_{12\_prime}(R) := \gamma_{2\_prime}(R) + \gamma_{3\_prime}(R)\cdot t_{22}(R) + \gamma_3(R)\cdot t_{22\_prime}(R)$$

The calculation of the derivatives of the Reflection and Transmission Coefficients with respect to R are provided:

$$dRc\_dR\_a(R) := \omega^2\cdot Z_2\cdot\left(t_{12}(R)\cdot t_{21\_prime}(R) - t_{12\_prime}(R)\cdot t_{21}(R) + t_{11\_prime}(R)\cdot t_{22}(R) - t_{11}(R)\cdot t_{22\_prime}(R)\right)$$

$$dRc\_dR\_b(R) := j\cdot\left[\omega^3\cdot Z_2^2\cdot\left(t_{11\_prime}(R)\cdot t_{12}(R) - t_{11}(R)\cdot t_{12\_prime}(R)\right) - \omega\cdot\left(t_{21\_prime}(R)\cdot t_{22}(R) - t_{21}(R)\cdot t_{22\_prime}(R)\right)\right]$$

$$dRc\_dR(R) := \frac{2\cdot Z_1\cdot\left(dRc\_dR\_a(R) + dRc\_dR\_b(R)\right)}{\left[\left(t_{21}(R) - \omega^2\cdot Z_1\cdot Z_2\cdot t_{12}(R)\right) + j\cdot\omega\cdot\left(t_{22}(R)\cdot Z_1 + t_{11}(R)\cdot Z_2\right)\right]^2} \quad = \quad \frac{\delta Rc}{\delta R}$$

$$dTc\_dR(R) := 2\cdot Z_1\cdot\left[\frac{\omega^2\cdot\left(t_{22\_prime}(R)\cdot Z_1 + t_{11\_prime}(R)\cdot Z_2\right) + j\cdot\left(\omega^3\cdot Z_1\cdot Z_2\cdot t_{12\_prime}(R) - \omega\cdot t_{21\_prime}(R)\right)}{\left[\left(t_{21}(R) - \omega^2\cdot Z_1\cdot Z_2\cdot t_{12}(R)\right) + j\cdot\omega\cdot\left(t_{22}(R)\cdot Z_1 + t_{11}(R)\cdot Z_2\right)\right]^2}\right] \quad = \quad \frac{\delta Tc}{\delta R}$$

The operation of the complex conjugate and the partial derivatives derivative are interchangeable, which leads to:

$$\frac{\delta\alpha}{\delta R} = -\left(dRc\_dR(R)\cdot\overline{R_c(R)} + R_c(R)\cdot\overline{dRc\_dR(R)}\right) - \frac{Z_2}{Z_1}\cdot\left(dTc\_dR(R)\cdot\overline{T_c(R)} + T_c(R)\cdot\overline{dTc\_dR(R)}\right)$$

50

Again, in order to complete a numerical analysis, a set of physical characteristics of the system must be input. In the case of this example, the previous values from Table 4-1 are used again with a concentration at the second resonance frequency of the baseline system. Evaluated at the higher of the two resonance frequencies:

$a := .0254 \cdot m$ $d := .1524 \cdot m$ $c := .1778 \cdot m$ $h := c + d$ $M_1 := 4.52 \cdot k$ $I_1 := \dfrac{M_1 \cdot (2 \cdot d)^2}{12}$

$b := .0254 \cdot m$ $f := .1524 \cdot m$ $e := .1778 \cdot m$ $l := e +$ $M_2 := 4.52 \cdot k$ $I_2 := \dfrac{M_2 \cdot (2 \cdot f)^2}{12}$

$\rho_1 := 1.144 \cdot \dfrac{kg}{m}$ $\rho_2 := 1.144 \cdot \dfrac{kg}{m}$ $Z_1 := 33.8231 \cdot \dfrac{kg}{sec}$ $Z_2 := 33.8231 \cdot \dfrac{kg}{sec}$ $K := 10 \cdot \dfrac{newton}{m}$ $\omega := 94.13 \cdot \dfrac{rad}{sec}$

$H := 1000 \cdot newton$ $T_{i\_minus} := \dfrac{Z_1^2}{\rho_1}$ $T_i := \dfrac{Z_2^2}{\rho_2}$

In order to obtain an initial estimate of the value of the damper for maximum absorption, a graph of the Power Adsorption Ratio is provided. This will provide the range for the initial estimate
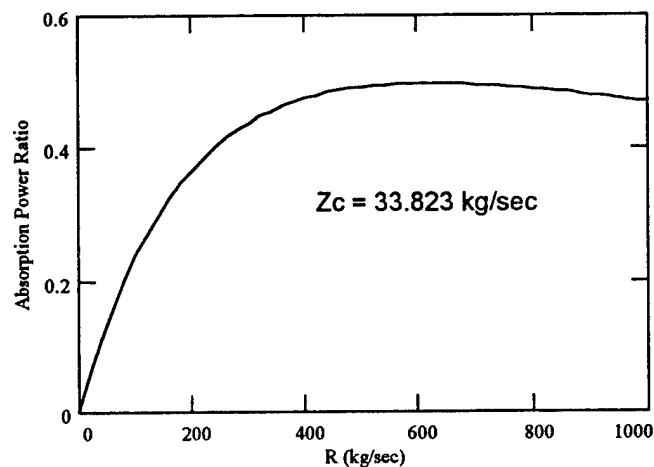
Figure B - 1: Plot of Absorption Power Ratio For Varying Values of R Using The Input Characteristics of Table 4 - 1

The expression to determine the optimum value for the damper is provided by:
The initial estimate is around 500 newton/(m/sec) from the graph above

$$R := 464.343 \cdot \frac{newton}{\frac{m}{sec}}$$

$$Best\_R := \left| root\left[-\left(dRc\_dR(R) \cdot \overline{R_c(R)} + R_c(R) \cdot \overline{dRc\_dR(R)}\right) \ldots \right. \right.$$
$$\left. \left. + -\left[\frac{Z_2}{Z_1} \cdot \left(dTc\_dR(R) \cdot \overline{T_c(R)} + T_c(R) \cdot \overline{dTc\_dR(R)}\right)\right] \right. , R \right] \right|$$

$$Best\_R = 464.343 \cdot \frac{newton}{\left(\frac{m}{sec}\right)}$$

This represents an iteration until the result was within three decimal places of the estimate. An iteration was performed until the solution was within three decimal places of

the initial estimate. The value of the optimum damper for this case is: 464.343 kg/sec.